

Lepton-flavor violating decays of neutral Higgs to muon and tauon in supersymmetric economical 3-3-1 model

P. T. Giang¹ L. T. Hue² D. T. Huong³ H. N. Long⁴

Institute of Physics, VAST, 10 Dao Tan, Ba Dinh, Hanoi, Vietnam

Abstract

We investigate Lepton-Flavor Violating (LFV) decays of Higgs to muon-tau in the supersymmetric economical 3-3-1 (SUSYE331) model. In the presence of flavor mixing in sleptons $\{\tilde{\mu}, \tilde{\tau}\}$ and large values of v/v' , the ratio of $Br(H \rightarrow \tau^+ \mu^-)/Br(H \rightarrow \tau^+ \tau^-)$ can reach to non-negligible values $\mathcal{O}(10^{-3})$, as in many known SUSY models. We predict that for the Standard Model Higgs boson, the LHC may detect its decay to muon and tauon. We also investigate the asymmetry between left and right LFV values of corrections and prove that the LFV effects are dominated by the left FLV term, which is $\mathcal{O}(10^3)$ times larger than the right LFV term in the limit of small values of $|\mu_\rho|/m_{SUSY}$. The contributions of Higgs-mediated effects to the decay $\tau \rightarrow \mu\mu\mu$ are also discussed.

Key words: Supersymmetric models, Decays of taus, Supersymmetric Higgs bosons

PACS: 12.60.Jv, 13.35.Dx, 14.80.Da

1 Introduction

The lepton flavor is absolutely conserved in the standard model (SM). Recently, experiments on neutrino oscillations have proved that lepton flavor is not conserved. It leads to motivation on a search for the signals of lepton flavor violations (LFV) beyond the SM. Many versions of the extension of Minimal

¹ Email: ptgiang@grad.iop.vast.ac.vn

² Email: lthue@iop.vast.ac.vn

³ Email: dthuong@iop.vast.ac.vn

⁴ Email: hnlong@iop.vast.ac.vn

Supersymmetric Standard Model (MSSM) with large $\tan\beta$ have been investigated in Higgs LFV decay. The interesting here is there exists parameter space that predicts the branching ratio of these types of decays are very sizable, enough to be detected by present colliders such as CERN Large Hadron Collider (LHC) [1] or International Linear Collider (ILC) [2]. For example, the SM [3] predicted that branching ratio of $H \rightarrow \mu\tau$ is very suppressed. However, in the beyond SM, this ratio can reach to large values, more than 10^{-4} . In particular, the refs. [4,5] showed that, in the MSSM, $BR(H \rightarrow \mu^+\tau^-) \sim 10^{-4}$ if $m_H/M_{SUSY} \sim 10^{-1}$. The Minimal Supersymmetric Neutrino Seesaw Models (ν MSSM) [6] predicted the branching ratio of heavy Higgs LFV decay is order of 10^{-4} while that of light Higgs LFV decay is order of 10^{-8} . For more discussions in details about the Higgs LFV decay, reader can found in [7,8,9,10,11] for MSSM, and ν MSSM, in [12] for little Higgs models (LTH).

The MSSM has shown that in the limit of large $\tan\beta$, the radiative corrections become non-negligible in many Higgs LFV decay processes. For example, refs. [7,9] showed that the ratio $R_{b/t} \equiv BR(H \rightarrow b\bar{b})/BR(H \rightarrow t\bar{t})$ can be distinguished between the MSSM and non-supersymmetric models. The main reason is that the Higgs boson couplings to down-type fermions receive a large corrections enhanced by $\tan\beta$. It leads to many interesting decay processes in quark sector such as $b \rightarrow s\gamma$ [13,14]. The large value of $\tan\beta$ also leads to many interesting effects in the lepton sector, especially when the LFV source in sleptons is included.

Recently, the Supersymmetric Economical 3-3-1 model (SUSYE331) has been constructed [15]. Apart from interesting features that mentioned in refs. [15,16,17,18], the scalar sector is minimal, and therefore it has been called the economical. In a series of works [15,16,17,18], we have developed and proved that the non-supersymmetric version [19] and supersymmetric version are consistent, realistic and very rich in physics. In the previous work [16], we skip the LFV source in the soft sector. However, the model predicts more interesting phenomenology if there exists LFV source in the soft breaking terms. In this paper, we will concentrate on LFV Higgs decays to $\mu\tau$ with the presence of misalignment of sleptons $\{\tilde{\mu}, \tilde{\tau}\}$ and their sneutrinos contained in soft breaking terms. In SUSYE331 model, for generating fermion masses as well as canceling anomaly, one needs four Higgs triplets. In particular, the "up" ρ^0 Higgs gives mass for neutrinos and the remain, "down" ρ'^0 , gives mass for charged leptons [15,17] and other Higgs give mass for quarks. The ρ^0 and ρ'^0 Higgs play very important roles if we consider effects of radiative correction in lepton sector in the limit of large $\tan\beta$. The corrections may cause many non-negligible effects, such as the correction of lepton mass, branching ratio of LFV Higgs decay...

In this work, we investigate the flavor violating Higgs coupling in SUSYE331 model, specially we focus on the $\{\mu, \tau\}$ generations.

Our work is arranged as follows: In section 2, we review the particle content in SUSYE331 model. The analytic expressions of the Higgs effective couplings are studied in section 3. In section 4, we study a numerical estimation on decay $H \rightarrow \mu\tau$ at colliders and compare contribution from the left and right LFV radiative corrections into the mentioned decay. In this section, we also consider the contributions of Higgs exchange to branching ratio of $\tau \rightarrow 3\mu$ decay. In the last section, we summarize our main results.

2 Particle content

Let us give brief report on the particle content in SUSYE331 model [15]. The superfields in the anomaly-free model are given by

$$\hat{L}_{aL} = (\hat{\nu}_a, \hat{l}_a, \hat{\nu}_a^c)^T \sim (1, 3, -1/3), \quad \hat{l}_{aL}^c \sim (1, 1, 1), \quad a = 1, 2, 3 \quad (1)$$

$$\hat{Q}_{1L} = (\hat{u}_1, \hat{d}_1, \hat{u}'^T)^T \sim (3, 3, 1/3), \quad (2)$$

$$\hat{u}_{1L}^c, \hat{u}'_{1L}^c \sim (3^*, 1, -2/3), \hat{d}_{1L}^c \sim (3^*, 1, 1/3), \quad (3)$$

$$\hat{Q}_{\alpha L} = (\hat{d}_\alpha, -\hat{u}_\alpha, \hat{d}'_\alpha)^T \sim (3, 3^*, 0), \quad \alpha = 2, 3, \quad (4)$$

$$\hat{u}_{\alpha L}^c \sim (3^*, 1, -2/3), \quad \hat{d}_{\alpha L}^c, \hat{d}'_{\alpha L}^c \sim (3^*, 1, 1/3), \quad (5)$$

$$\hat{\chi} = (\hat{\chi}_1^0, \hat{\chi}^-, \hat{\chi}_2^0)^T \sim (1, 3, -1/3), \quad \hat{\rho} = (\hat{\rho}_1^+, \hat{\rho}^0, \hat{\rho}_2^+)^T \sim (1, 3, 2/3), \quad (6)$$

$$\hat{\chi}' = (\hat{\chi}'^o, \hat{\chi}'^+, \hat{\chi}'^o)^T \sim (1, 3^*, 1/3), \quad \hat{\rho}' = (\hat{\rho}'^-, \hat{\rho}'^o, \hat{\rho}'^+)^T \sim (1, 3^*, -2/3). \quad (7)$$

Here we use some new notations as $\hat{\psi}_L^c = (\hat{\psi}_R)^c \equiv \hat{\psi}_R^\dagger$ and exotic quarks are denoted by usual quarks with prime-superscripts (u' with the electric charge $q_{u'} = 2/3$ and d' with $q_{d'} = -1/3$). The values in each parenthesis show corresponding quantum numbers of the $(SU(3)_c, SU(3)_L, U(1)_X)$ symmetry. In this model, the $SU(3)_L \otimes U(1)_X$ gauge group is broken via two steps:

$$SU(3)_L \otimes U(1)_X \xrightarrow{w, w'} SU(2)_L \otimes U(1)_Y \xrightarrow{v, v', u, u'} U(1)_Q, \quad (8)$$

where the VEVs are defined by

$$\sqrt{2}\langle\chi\rangle^T = (u, 0, w), \quad \sqrt{2}\langle\chi'\rangle^T = (u', 0, w') \quad (9)$$

$$\sqrt{2}\langle\rho\rangle^T = (0, v, 0), \quad \sqrt{2}\langle\rho'\rangle^T = (0, v', 0). \quad (10)$$

The vector superfields \widehat{V}_c , \widehat{V} and \widehat{V}' containing the usual gauge bosons are given in [15,17]. The supersymmetric model possessing a general Lagrangian is studied in [17]. In the following, only terms relevant to our calculations are displayed.

3 Higgs-muon-tauon effective interactions

In the SUSYE331 model [15,17], at the tree level, the down-type leptons (e, μ, τ) only couple to the neutral Higgs (ρ^0) through the Yukawa interaction given by

$$\mathcal{L}_{lH} = -\frac{\lambda_{lab}}{3}(L_{aL}l_{bL}^c\rho^0 + \text{H.c}). \quad (11)$$

In general case, $\lambda_{lab} \neq 0$, the Lagrangian given in (11) not only provides mass for the charged leptons but also gives the source of the lepton flavor mixing at the tree level. It means that if the couplings $\lambda_{lab} \neq 0$ with ($a \neq b$), the LFV processes, such as $\text{Higgs} \rightarrow \mu\tau$, must be existed. In this case, our theory predicts very large branching ratios of LFV processes which exceed to experimental results discussed in [20]. Hence, in the following calculation, we skip the λ_{lab} with ($a \neq b$) in (11).

Let us consider another source of LFV which is caused by slepton mixing. For more details of slepton mixing, ones can find in Appendix C. Because of slepton mixing, the leading effective interactions of leptons with ρ^o, ρ'^o Higgs can be appeared at the one-loop order. In this paper, we will concentrate only on the couplings of Higgs with $\{\mu, \tau\}$ leptons.

In order to consider the μ, τ flavor mixing at the one loop level, first we rewrite the original Lagrangian (11) in terms of two component spinor notations which are familiar to those in literature, namely

$$-\mathcal{L}_{0\mu\tau} = (Y_\mu\mu_L^c\mu_L + Y_\tau\tau_L^c\tau_L)\rho^0 + \text{H.c}, \quad (12)$$

where $Y_\mu \equiv \lambda_{122}/3, Y_\tau \equiv \lambda_{133}/3$.

At the one-loop level, if we skip all of the terms which are proportional to Y_μ except terms contributing to mass of muon, then Yukawa interactions containing Higgs-lepton-lepton couplings can be divided into two parts:

- The lepton-flavor conversing (LFC) part given by

$$-\Delta\mathcal{L}_{FC} = (Y_\mu\Delta_\mu^{1\rho} + Y_\tau\Delta_\mu^{2\rho})\mu_L^c\mu_L\rho^{0*} + Y_\tau\Delta_\tau^\rho\tau_L^c\tau_L\rho^{0*}$$

$$+ (Y_\mu \Delta_\mu^{1\rho'} + Y_\tau \Delta_\mu^{2\rho'}) \mu_L^c \mu_L \rho'^0 + Y_\tau \Delta_\tau^{\rho'} \tau_L^c \tau_L \rho'^0 + \text{H.c.}, \quad (13)$$

- The lepton-flavor violating (LFV) part given as

$$\begin{aligned} -\Delta \mathcal{L}_{FV} = & Y_\tau (\Delta_L^\rho \tau_L^c \mu_L + \Delta_R^\rho \mu_L^c \tau_L) \rho^{0*} \\ & + Y_\tau (\Delta_L^{\rho'} \tau_L^c \mu_L + \Delta_R^{\rho'} \mu_L^c \tau_L) \rho'^0 + \text{H.c.}, \end{aligned} \quad (14)$$

where all of $\Delta_\mu^{1\rho}, \Delta_\mu^{2\rho}, \Delta_\mu^{1\rho'}, \Delta_\mu^{2\rho'}, \Delta_\tau^\rho, \Delta_\tau^{\rho'}, \Delta_L^\rho, \Delta_L^{\rho'}, \Delta_R^\rho$ and $\Delta_R^{\rho'}$ are the leading effective couplings.

From now on, for convenience, we use notation Δ to imply any radiative correction of couplings appearing in (13) and (14). Note that Δ is a dimensionless function of mass parameters and $\Delta_\mu^\rho, \Delta_\tau^\rho$ are non-zero value even if we assume that there is no flavor mixing in slepton sector. We emphasize that Δ_τ^ρ is one of quantities affecting on many observable quantities such as the ratio of branching ratios $Br(H \rightarrow b\bar{b})/BR(H \rightarrow \tau\bar{\tau})$. The contribution of Δ_τ^ρ to that of branching ratios in the SUSY model is studied in [7,9]. The diagrams which contribute to all of Δ s are drawn in Appendix A.

Now let us construct the total effective Lagrangian for Higgs, muon and tauon couplings in terms of physical eigenstates. First we write down the whole Lagrangian coming from all of Eqs. (12), (13) and (14) in the matrix form

$$-\mathcal{L} = Y_\tau \begin{pmatrix} \mu_L^c & \tau_L^c \end{pmatrix} \mathcal{Y}_{l_1} \begin{pmatrix} \mu_L \\ \tau_L \end{pmatrix} \rho'^0 + Y_\tau \begin{pmatrix} \mu_L^c & \tau_L^c \end{pmatrix} \mathcal{Y}_{l_2} \begin{pmatrix} \mu_L \\ \tau_L \end{pmatrix} \rho^{0*} + \text{H.c.}, \quad (15)$$

where \mathcal{Y}_{l_1} and \mathcal{Y}_{l_2} are matrices defined by the following formulas:

$$\mathcal{Y}_{l_1} = \begin{pmatrix} \Delta_\mu^{o\rho'} & \Delta_R^{\rho'} \\ \Delta_L^{\rho'} & 1 + \Delta_\tau^{\rho'} \end{pmatrix}; \quad \mathcal{Y}_{l_2} = \begin{pmatrix} \Delta_\mu^{o\rho} & \Delta_R^\rho \\ \Delta_L^\rho & \Delta_\tau^\rho \end{pmatrix}, \quad (16)$$

with $y \equiv Y_\mu/Y_\tau$, $\Delta_\mu^{o\rho} \equiv y\Delta_\mu^{1\rho} + \Delta_\mu^{2\rho}$ and $\Delta_\mu^{o\rho'} \equiv y + y\Delta_\mu^{1\rho'} + \Delta_\mu^{2\rho'}$.

Because of loop corrections, the mass matrix of the μ, τ in (15) is no longer diagonal. In order to find the physical eigenstates of muon and tauon, we expand the Higgs ρ and ρ' around the vacuum expectation values. As a consequence, the mixing mass matrix for the muon and tauon are

$$-\mathcal{L}_{mass} = Y_\tau v' \begin{pmatrix} \mu_L^c & \tau_L^c \end{pmatrix} \mathcal{Y}_l \begin{pmatrix} \mu_L \\ \tau_L \end{pmatrix} + \text{H.c.}, \quad (17)$$

where

$$\begin{aligned}
\mathcal{Y}_l &\equiv \mathcal{Y}_{l_1} + t_\gamma \mathcal{Y}_{l_2} = (1 + \Delta_\tau^{\rho'} + \Delta_\tau^\rho t_\gamma) \begin{pmatrix} \epsilon_\mu & \epsilon_R \\ \epsilon_L & 1 \end{pmatrix} \\
&= (1 + \Delta_\tau^{\rho'} + \Delta_\tau^\rho t_\gamma) Y_\epsilon,
\end{aligned} \tag{18}$$

with

$$\begin{aligned}
t_\gamma &\equiv \tan \gamma = \frac{v}{v'} = \frac{\langle \rho^0 \rangle}{\langle \rho'^0 \rangle}, \quad \epsilon_\mu \equiv \frac{\Delta_\mu^{o\rho'} + \Delta_\mu^{o\rho} t_\gamma}{1 + \Delta_\tau^{\rho'} + \Delta_\tau^\rho t_\gamma}, \\
\epsilon_L &\equiv \frac{\Delta_L^{\rho'} + \Delta_L^\rho t_\gamma}{1 + \Delta_\tau^{\rho'} + \Delta_\tau^\rho t_\gamma}, \quad \epsilon_R \equiv \frac{\Delta_R^{\rho'} + \Delta_R^\rho t_\gamma}{1 + \Delta_\tau^{\rho'} + \Delta_\tau^\rho t_\gamma}
\end{aligned} \tag{19}$$

and

$$Y_\epsilon = \begin{pmatrix} \epsilon_\mu & \epsilon_R \\ \epsilon_L & 1 \end{pmatrix} \tag{20}$$

It is easy to see that the mixing mass matrix of muon and tauon given in (20) is a general matrix. Finding the mass eigenvalues of left-right leptons is equivalent to finding a matrix C satisfying:

$$C^\dagger \mathcal{Y}_\epsilon^\dagger \mathcal{Y}_\epsilon C = \begin{pmatrix} y_\mu^2 & 0 \\ 0 & y_\tau^2 \end{pmatrix} \equiv \mathcal{Y}_d^2, \tag{21}$$

In our theory, the matrix C can be found in a form

$$C = \begin{pmatrix} c_\Lambda & s_\Lambda \\ -s_\Lambda & c_\Lambda \end{pmatrix}, \tag{22}$$

where $c_\Lambda \equiv \cos \Lambda$, $s_\Lambda \equiv \sin \Lambda$ and Λ is the rotation angle given by

$$t_{2\Lambda} \equiv \tan(2\Lambda) = \frac{2(\epsilon_\mu \epsilon_R + \epsilon_L)}{1 + \epsilon_R^2 - (\epsilon_\mu^2 + \epsilon_L^2)}. \tag{23}$$

In addition, $\mathcal{Y}_d = \text{diag}(y_\mu, y_\tau)$ in which (y_μ, y_τ) are defined as follows

$$y_\mu^2 = r' - r s_\Lambda^2, \quad y_\tau^2 = r' + r c_\Lambda^2, \tag{24}$$

where

$$r^2 \equiv 4(\epsilon_\mu \epsilon_R + \epsilon_L)^2 + \left[1 + \epsilon_R^2 - (\epsilon_\mu^2 + \epsilon_L^2)\right]^2, \quad r' \equiv \epsilon_\mu^2 + \epsilon_L^2. \quad (25)$$

Note that the mass eigenvalues of muon and tauon are proportional to (y_μ, y_τ) , namely

$$m_\mu = y_\mu Y_\tau v'(1 + \Delta_\tau^{\rho'} + \Delta_\tau^\rho), \quad m_\tau = y_\tau Y_\tau v'(1 + \Delta_\tau^{\rho'} + \Delta_\tau^\rho). \quad (26)$$

On the other hand, the mass eigenstates of leptons (μ, τ) and (μ^c, τ^c) are determined from two transformations

$$\begin{aligned} L^c &= \begin{pmatrix} \mu^c \\ \tau^c \end{pmatrix} = (U_l)^T \begin{pmatrix} \mu_L^c \\ \tau_L^c \end{pmatrix} = U_l^T L_L^c, \\ L &= \begin{pmatrix} \mu \\ \tau \end{pmatrix} = V_l \begin{pmatrix} \mu_L \\ \tau_L \end{pmatrix} = V_l L_L. \end{aligned} \quad (27)$$

where U_l and V_l have come from (21), namely

$$\begin{aligned} U_l^\dagger &= \mathcal{Y}_d^{-1} C^\dagger \mathcal{Y}_\epsilon^\dagger = \begin{pmatrix} \frac{1}{y_\mu} & 0 \\ 0 & \frac{1}{y_\tau} \end{pmatrix} \begin{pmatrix} c_\Lambda & -s_\Lambda \\ s_\Lambda & c_\Lambda \end{pmatrix} \begin{pmatrix} \epsilon_\mu & \epsilon_L \\ \epsilon_R & 1 \end{pmatrix}, \\ V_l^\dagger &= C = \begin{pmatrix} c_\Lambda & s_\Lambda \\ -s_\Lambda & c_\Lambda \end{pmatrix}. \end{aligned} \quad (28)$$

Next, we replace \mathcal{Y}_{l_1} in Eq. (15) by a new form deduced from Eq.(18)

$$\mathcal{Y}_{l_1} = (1 + \Delta_\tau^{\rho'} + \Delta_\tau^\rho t_\gamma) Y_\epsilon - \mathcal{Y}_{l_2} t_\gamma$$

Now we have obtained a new expression of (15) as follows

$$\begin{aligned} -\mathcal{L} &= Y_\tau (1 + \Delta_\tau^{\rho'} + \Delta_\tau^\rho t_\gamma) \begin{pmatrix} \mu_L^c & \tau_L^c \end{pmatrix} \mathcal{Y}_\epsilon \begin{pmatrix} \mu_L \\ \tau_L \end{pmatrix} \rho'^o \\ &\quad + Y_\tau \begin{pmatrix} \mu_L^c & \tau_L^c \end{pmatrix} \mathcal{Y}_{l_2} \begin{pmatrix} \mu_L \\ \tau_L \end{pmatrix} (\rho^{o*} - t_\gamma \rho'^o) + \text{H.c.}, \end{aligned} \quad (29)$$

In the basis of mass eigenstates of the muon and tauon given in Eq. (27), the Lagrangian (29) transforms into

$$\begin{aligned}
- \mathcal{L}_d = & Y_\tau (1 + \Delta_\tau^{\rho'} + \Delta_\tau^\rho t_\gamma) L^{cT} \mathcal{Y}_d L \rho'^o \\
& + Y_\tau L^{cT} (U_l^\dagger \mathcal{Y}_2 V_l^\dagger) L (\rho^{o*} - t_\gamma \rho'^o) + \text{H.c.}
\end{aligned} \tag{30}$$

It is needed to emphasize that the first term in Eq. (30) generates only masses for muon and tauon while the second creates masses as well as give rise to the lepton flavor mixing. Sources of flavor mixing are two off-diagonal elements of the matrix $(U_l^\dagger \mathcal{Y}_2 V_l^\dagger)$:

$$\begin{aligned}
(U_l^\dagger \mathcal{Y}_2 V^\dagger)_{12} = & \frac{c_\Lambda^2 \Delta_R^\rho \epsilon_\mu}{y_\mu} + \frac{(c_\Lambda^2 \epsilon_L - c_\Lambda s_\Lambda) \Delta_\tau^\rho}{y_\mu} \\
& + \frac{c_\Lambda s_\Lambda (\Delta_L^\rho \epsilon_L + \Delta_\mu^{o\rho} \epsilon_\mu - \Delta_R^\rho \epsilon_R) - s_\Lambda^2 (\Delta_L^\rho + \epsilon_R \Delta_R^\rho)}{y_\mu},
\end{aligned} \tag{31}$$

$$\begin{aligned}
(U_l^\dagger \mathcal{Y}_2 V^\dagger)_{21} = & \frac{c_\Lambda^2 \Delta_L^\rho}{y_\tau} + \frac{c_\Lambda^2 \Delta_\mu^{o\rho} \epsilon_R - c_\Lambda s_\Lambda \Delta_\tau^\rho}{y_\tau} \\
& + \frac{c_\Lambda s_\Lambda (\Delta_L^\rho \epsilon_L + \Delta_\mu^{o\rho} \epsilon_\mu - \Delta_R^\rho \epsilon_R) - s_\Lambda^2 (\Delta_\tau^\rho \epsilon_L + \epsilon_\mu \Delta_R^\rho)}{y_\tau}
\end{aligned} \tag{32}$$

In the further calculations, we consider a case of $(t_\gamma \Delta) \ll 1$ but large enough (as investigated in MSSM) to cause many interesting effects, and we will comment more details after some numerical calculations. On the other hand, the rotation angle given in Eq. (23) is very small, so we can set $c_\Lambda \simeq 1$, $s_\Lambda \simeq \Lambda$. As a result, the Eqs. (24), (31) and (32) can be presented as very simple formulas:

$$\begin{aligned}
y_\mu \simeq \epsilon_\mu, \quad y_\tau \simeq 1, \\
(U_l^\dagger \mathcal{Y}_2 V^\dagger)_{12} \simeq \Delta_R^\rho, \quad (U_l^\dagger \mathcal{Y}_2 V^\dagger)_{21} \simeq \Delta_L^\rho.
\end{aligned} \tag{33}$$

and the above LFV Lagrangian also appears in a simple form:

$$- \mathcal{L}_{FV} \simeq Y_\tau (\Delta_R^\rho \mu^c \tau + \Delta_L^\rho \tau^c \mu) (\rho^{0*} - t_\gamma \rho^0) + \text{H.c.} \tag{34}$$

Finally, in the mass-eigenstate basis for both lepton and Higgs, we obtain the effective LFV Lagrangian:

$$- \mathcal{L}_{FV} \simeq \sqrt{2} Y_\tau (\Delta_R^\rho \mu^c \tau + \Delta_L^\rho \tau^c \mu) (s_\alpha s_\gamma \phi_{S_{a36}} - c_\alpha s_\gamma \varphi_{S_{a36}}) + \text{H.c.}, \tag{35}$$

where $\varphi_{S_{a36}}$ and $\phi_{S_{a36}}$ are the Higgs mass eigenstates generated from the mixing of two original Higgs bosons ρ^0 and ρ'^0 . The expressions of the Higgs mass eigenstates were introduced in [17]. They are summarized in the appendix C. The emphasis here is that in the general supersymmetric model there exist both the leading interactions of the muon, tauon with neutral scalar and

pseudo scalar Higgs. However, the SUSYE331 model contains only interactions among muon, tauon and scalar Higgs.

The effective couplings given in (35) are widely investigated for many LFV low-energy processes, specially in the MSSM [4,10,21]. In this paper we first concentrate on some simple aspects of LFV in the SUSYE331 model. In particular, we are going to consider the LFV in decays of the scalar Higgs, i.e $\Phi^0 \rightarrow \tau^\pm \mu^\mp$, where $\Phi^0 = \varphi_{S_{a36}}$ or $\phi_{S_{a36}}$. First, we start with studying the branching ratios of neutral Higgs decay into muon and tauon. The SUSYE331 model predicts that the formula of these branching ratios is

$$\begin{aligned} BR(\Phi^0 \rightarrow \tau^+ \mu^-) &= BR(\Phi^0 \rightarrow \tau^- \mu^+) \\ &= 2(1 + \tan^2 \gamma) \left(|\Delta_L^\rho|^2 + |\Delta_R^\rho|^2 \right) BR(\Phi^0 \rightarrow \tau^+ \tau^-). \end{aligned} \quad (36)$$

This result is similar to that one given in [4], except the absence of angle of mixing among Higgses. In the limit of appropriately large $\tan \gamma$, the effects of LFV in the Higgs decay processes is not to be ignored. Hence, our theoretical prediction is not much different from that of previous results given in [4,5,7,8,21]. For details, we will study some numerical calculations for the branching ratios indicated by Eq.(36). In our paper, we use the assumption for slepton mixing presented in appendix C. The diagrams giving contributions to Δ_R^ρ and Δ_L^ρ are shown in Fig.1. The relevant vertices to our calculation are presented in appendix B.

Using Feymann rules, we can obtain the expression Δ_L^ρ from the diagrams in Fig.1, namely:

$$\Delta_L^\rho = \Delta_{La}^\rho + \Delta_{Lb}^\rho + \Delta_{Lc}^\rho + \Delta_{Ld}^\rho + \Delta_{Le}^\rho + \Delta_{Lf}^\rho + \Delta_{Lk}^\rho, \quad (37)$$

where

$$\begin{aligned} \Delta_{La}^\rho &= \frac{g'^2}{216\pi^2} \mu_\rho m' c_L s_L \left[I_3(m'^2, \mu_\rho^2, \tilde{m}_{L_2}^2) - I_3(m'^2, \mu_\rho^2, \tilde{m}_{L_3}^2) \right], \\ \Delta_{Lb}^\rho &= -\frac{g^2}{24\pi^2} \mu_\rho m_\lambda c_L s_L \left[I_3(m_\lambda^2, \mu_\rho^2, \tilde{m}_{L_2}^2) - I_3(m_\lambda^2, \mu_\rho^2, \tilde{m}_{L_3}^2) \right], \\ \Delta_{Lc}^\rho &= -\frac{g^2}{16\pi^2} \mu_\rho m_\lambda c_{\nu_L} s_{\nu_L} \left[I_3(m_\lambda^2, \mu_\rho^2, \tilde{m}_{\nu_{L2}}^2) - I_3(m_\lambda^2, \mu_\rho^2, \tilde{m}_{\nu_{L3}}^2) \right], \\ \Delta_{Ld}^\rho &= -\frac{g^2}{16\pi^2} \mu_\rho m_\lambda c_{\nu_R} s_{\nu_R} \left[I_3(m_\lambda^2, \mu_\rho^2, \tilde{m}_{\nu_{R2}}^2) - I_3(m_\lambda^2, \mu_\rho^2, \tilde{m}_{\nu_{R3}}^2) \right], \\ \Delta_{Le}^\rho &= \frac{(Y_{\nu_{\mu\tau}}) h_{\mu\tau} - h_{\tau\mu} \mu_\rho}{8\pi^2} \end{aligned}$$

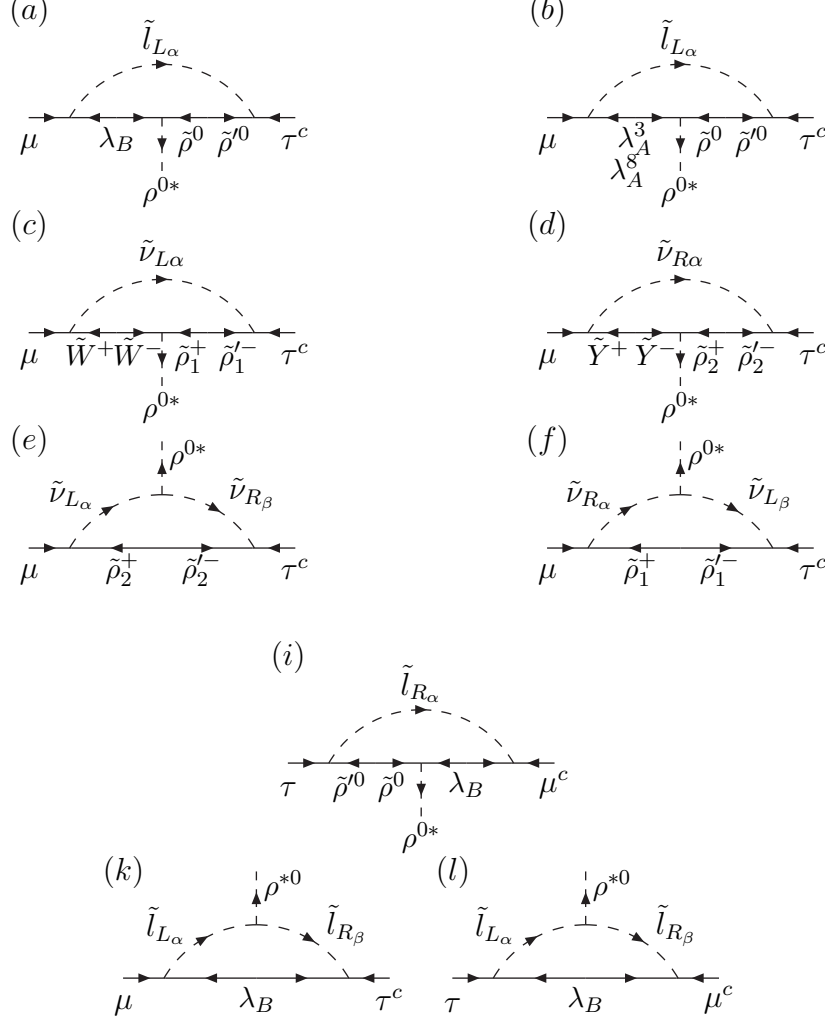


Fig. 1. Diagrams contributing to Δ_L^ρ [(a), (b), (c), (d), (e), (f), (k)] and Δ_R^ρ [(i), (l)].

$$\begin{aligned}
& \times \left[s_{\nu_{(L-R)}} \left(s_{\nu_L} s_{\nu_R} I_3(\mu_\rho^2, \tilde{m}_{\nu_{L2}}^2, \tilde{m}_{\nu_{R2}}^2) + c_{\nu_L} c_{\nu_R} I_3(\mu_\rho^2, \tilde{m}_{\nu_{L3}}^2, \tilde{m}_{\nu_{R3}}^2) \right) \right. \\
& \left. + c_{\nu_{(L-R)}} \left(s_{\nu_R} c_{\nu_L} I_3(\mu_\rho^2, \tilde{m}_{\nu_{L2}}^2, \tilde{m}_{\nu_{R2}}^2) - s_{\nu_L} c_{\nu_R} I_3(\mu_\rho^2, \tilde{m}_{\nu_{L2}}^2, \tilde{m}_{\nu_{R3}}^2) \right) \right], \\
\Delta_{Lf}^\rho &= -\Delta_{Le}^\rho, \\
\Delta_{Lk}^\rho &= \frac{g'^2}{288\pi^2} \mu_\rho m' s_L c_L \left[s_R^2 \left(I_3(m'^2, \tilde{m}_{L2}^2, \tilde{m}_{R2}^2) - I_3(m'^2, \tilde{m}_{L3}^2, \tilde{m}_{R2}^2) \right) \right. \\
& \left. + c_R^2 \left(I_3(m'^2, \tilde{m}_{L2}^2, \tilde{m}_{R3}^2) - I_3(m'^2, \tilde{m}_{L3}^2, \tilde{m}_{R3}^2) \right) \right]. \tag{38}
\end{aligned}$$

Also, the Δ_R^ρ receives contributions from two diagrams (i) and (l) of Fig.1 too,

$$\Delta_R^\rho = \Delta_{Ri}^\rho + \Delta_{Rl}^\rho, \tag{39}$$

where

$$\begin{aligned}
\Delta_{Ri}^\rho &= -\frac{g'^2}{72\pi^2} \mu_\rho m' c_R s_R \left[I_3(m'^2, \mu_\rho^2, \tilde{m}_{R_2}^2) - I_3(m'^2, \mu_\rho^2, \tilde{m}_{R_3}^2) \right], \\
\Delta_{Rl}^\rho &= \frac{g'^2}{288\pi^2} \mu_\rho m' s_R c_R \left[s_L^2 \left(I_3(m'^2, \tilde{m}_{L_2}^2, \tilde{m}_{R_2}^2) - I_3(m'^2, \tilde{m}_{L_2}^2, \tilde{m}_{R_3}^2) \right) \right. \\
&\quad \left. + c_L^2 \left(I_3(m'^2, \tilde{m}_{L_3}^2, \tilde{m}_{R_2}^2) - I_3(m'^2, \tilde{m}_{L_3}^2, \tilde{m}_{R_3}^2) \right) \right]
\end{aligned} \tag{40}$$

Here we have used some new notations

$$s_{\nu(L-R)} \equiv s_{\nu_L} c_{\nu_R} - s_{\nu_R} c_{\nu_L}, \quad c_{\nu(L-R)} \equiv s_{\nu_L} s_{\nu_R} + c_{\nu_L} c_{\nu_R}, \tag{41}$$

where s_L , c_L and s_R , c_R are deduced from mixing angles for left and right handed sleptons (for details, see Appendix C.2). The same relations hold for sneutrino sector, with corresponding notations for mixing angles s_{ν_L} , s_{ν_R} , c_{ν_L} and c_{ν_R} . The function $I_3(x, y, z)$ is similar to that mentioned in literature [5],

$$I_3(x, y, z) = \frac{xy \log(x/y) + yz \log(y/z) + zx \log(z/x)}{(x-y)(y-z)(z-x)}. \tag{42}$$

The analytical results appearing in (38) show that contributions from two diagrams (e) and (f) to the Δ_L^ρ always are the same magnitude but opposite in sign. Therefore the total contribution of these two diagrams to Δ_L^ρ vanishes. On the other hand, results obtained from the Eq.(38) show that if we neglect the terms of the slepton mixing, namely $s_L = s_R = s_{\nu_L} = s_{\nu_R} = 0$, the amounts collected from the $\Delta_{L,R}^\rho$ class diagrams given in Fig. 1 are all zero. This corresponds to the case of lepton flavor conservation: $\Delta_L^\rho = \Delta_R^\rho = 0$.

We also remind that analytical expressions of other Δ functions can be found in Appendix A. These results demonstrate that the values $\Delta_\mu^{1\rho}$, $\Delta_\mu^{2\rho}$ and Δ_τ^ρ given by expressions (A.1), (A.2) and (A.3) obtained at one loop approximation, do not vanish even if we assume no mixing of the sleptons. These quantities create non-negligible effects of the lepton masses. They are widely discussed in many previous papers. Another feature of the SUSYE331 model that we would like to remind here: there are two independent sources (Yukawa coupling at tree level) to create masses of slepton and neutrino sectors. Hence, contributions to LFV corrections come from two independent sources: mixing of lepton and sneutrino sectors. We assume that the model contains both LFV sources.

Before coming to numerical computation section, it is necessary to note that the formulas of LFV corrections, such as Δ s in this case, have not been established for the SUSYE331 model before. So let us give some general comments on the formulas of Δ s which discriminate against those in MSSM versions:

- At the one loop approximation, the effective couplings Δ s are obtained from

the diagrams such as those listed in Figs. (A.1) and (A.2). We can distinguish two types of diagram which give contribution to Δ s. The first type of diagram does not include any Higgsino propagators, for examples Figs. 1 (*k*) and (*l*), and they are known as pure gaugino-mediated diagrams. The second, containing at least one Higgsino propagator like remaining diagrams, is Higgsino-mediated type. In general case, each of these kinds of diagram may give main contribution to the Δ s depending on regions of mass parameter space. If each Higgsino-mediated diagram gives the dominated contribution to Δ s that reach to single maximum value. In contrast, each Δ that gains values from pure gaugino-mediated diagrams, Δ_{Lk}^ρ for example, is proportional to $|\mu_\rho|$. Additionally, we can see the analytic expressions of Δ s given in (38), (40) and appendix A. It is well known in beyond MSSM theories [4], all of effective couplings Δ s are obtained from both types of diagrams, except Δ'_μ . In the limit of large values of $|\mu_\rho|$, the dominated contributions of Δ s are caused by pure gaugino-mediated diagrams. This conclusion also is happened in the SUSYE331. However, in the SUSYE331, there are the additional $SU(3)_L$ gaugino-mediated diagrams. Hence the values of Δ_L^ρ can be changed in comparison with other models. Details of this difference are discussed in section 4.

- The difference between the predictions of the model under consideration and other ones due to hypercharge structure of particle content. For example, let us compare our expressions of Δ s with those of Δ s in MSMS [4]. All contributions to the Δ s obtained from Fig.1, are proportional to I_3 functions. Rate coefficients in both models are the same level for diagrams of Higgsino-mediated type whereas the rate coefficients in the model under consideration are smaller than that in the MSSM model for diagrams of pure gaugino-mediated type. As a consequence, the large contribution to the Δ s from the pure gaugino-mediated type will happen if mass parameters are large. Furthermore, in this limit of mass parameters, the pure gaugino-mediated diagrams are the only source giving contribution to radiative corrections $\Delta_\mu^{2\rho}$ of muon mass. It is nature to keep the ratio Y_τ/Y_μ , at one loop correction, to be the same as those at tree level. This leads to the limit of the mass parameters, which does not exceed 10 TeV .

In the next section we will investigate some numerical results. On that basis, we will compare the effects of the LFV origin in the left and right slepton sectors as well as sneutrino sectors. In order to investigate numerically, we are going to use results from [17] such as: $g'/g = \frac{3\sqrt{2}s_W}{\sqrt{4c_W^2-1}}$, $s_W^2 = 0.2312$ and $\alpha_{em}^{-1} = 128$ at the weak scale.

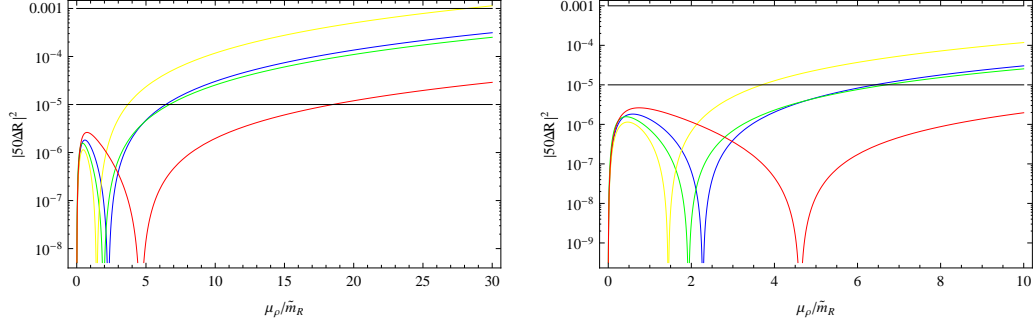


Fig. 2. $|\Delta_R^\rho|^2$ as a function of $|\mu_\rho|/\tilde{m}_R$ with four different choices of masses ratios: 1) blue curve $m' = \tilde{m}_R = \tilde{m}_L$; 2) green curve $3m' = \tilde{m}_R = \tilde{m}_L$; 3) yellow curve $m' = \tilde{m}_R = 3\tilde{m}_L$; 4) red curve $m' = \tilde{m}_R = \tilde{m}_L/3$. Two black lines correspond to two values 10^{-5} and 10^{-3} of $|50\Delta_R^\rho|^2$.

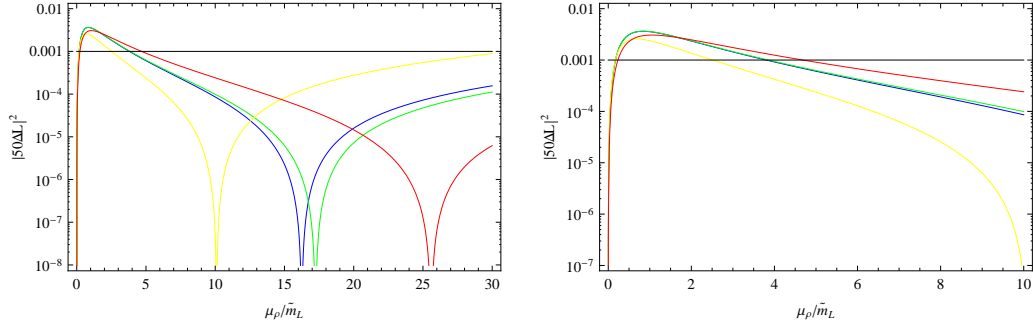


Fig. 3. $|\Delta_L^\rho|^2$ as a function of $|\mu_\rho|/\tilde{m}_L$ with four different choices of masses ratios: 1) blue curve $m' = \tilde{m}_R = \tilde{m}_L$; 2) green curve $3m' = \tilde{m}_R = \tilde{m}_L$; 3) yellow curve $m' = \tilde{m}_L = 3\tilde{m}_R$; 4) red curve $m' = \tilde{m}_L = \tilde{m}_R/3$. A black line corresponds to value 10^{-3} of $|50\Delta_L^\rho|^2$.

4 Numerical results

In this section we firstly discuss some numerical results that relate to any signals of LFV decays $H \rightarrow \mu\tau$. Let us start with the maximum LFV in both left and right sectors, especially $s_L c_L = s_R c_R = s_{\nu_L} c_{\nu_L} = s_{\nu_R} c_{\nu_R} = 0.5$. It means that we can assign values of mass parameters like:

$$\begin{aligned}\tilde{m}_{(\tau_L, \tau_R, \nu_{\tau_L}, \nu_{\tau_R})}^2 &= \tilde{m}_{(\mu_L, \mu_R, \nu_{\mu_L}, \nu_{\mu_R})}^2 \\ &= \tilde{m}_{L,R,\nu_L,\nu_R}^2, \\ \tilde{m}_{(L_2, R_2, \nu_{L_2}, \nu_{R_2})}^2 &= 0.2 \tilde{m}_{L,R,\nu_L,\nu_L}^2\end{aligned}$$

and

$$\tilde{m}_{(L_3, R_3, \nu_{L_3}, \nu_{R_3})}^2 = 1.8 \tilde{m}_{(L,R,\nu_L,\nu_R)}^2,$$

where $\tilde{m}_{(L,R,\nu_L,\nu_R)}^2$ are mass parameters used to compare with SUSY mass scale

m_{SUSY} . We would like to emphasize that branching ratios of Higgs decays to muon and tauon are sizable if $\tan \gamma$ is large enough. Therefore, in the following calculations, we take $\tan \gamma \sim 50$.

The Fig.2 displays the quantity $|50\Delta_R^\rho|^2$ as a function of $|\mu_\rho|/\tilde{m}_R$ while the Fig.3 displays the $|50\Delta_L^\rho|^2$ as a function of $|\mu_\rho|/\tilde{m}_L$ where all other relevant parameters are fixed. Each curve presented in the Figs.2, 3 contains a single peak. All the peaks of the curves are obtained at mass parameters at which the contribution of the Higgs-mediated diagrams to Δ s are dominated. Corresponding to each curve, there are two regions of mass parameter space separated by deep wells. Deep wells, which divide the parameter space into two parts. The first part, the mass parameters are located in the right hand side of deep wells. In this region of parameter space, the pure gaugino-mediated type can give main contribution to Δ s. The second part, the mass parameters are located in the left handed side of deep wells at which the dominated contribution to Δ s is obtained by the Higgs-mediated. All of the maximum points of the curves in the Fig.2 and Fig.3 are reached at $|\mu_\rho|/\tilde{m}_{L,R} \sim \mathcal{O}(10^{-1})$ and these values depend weakly on the changes of values of \tilde{m}_L and \tilde{m}_R . On the other hand, the maximum values of the Δ_L^ρ is $\mathcal{O}(10^{-3})$, as concerned in the MSSM [4,6,10,22] while the maximum values of the Δ_R^ρ are much smaller than of Δ_L^ρ , specially $\max(|\Delta_R^\rho|)^2/\max(|\Delta_L^\rho|)^2 \sim 10^{-3}$. This large difference comes from the symmetry of $SU(3)_L \times U(1)_X$ model. In particular, in the left-side of wells the main contributions to Δ_L^ρ of SUSYE331 model come from the $SU(3)_L$ gaugino-mediated diagrams, namely diagrams (b,c,d) in Fig.1. In contrast, the main contributions to Δ_R^ρ come from only $U(1)$ gaugino-mediated diagram. Figs.2 and 3 also show that both Δ_L^ρ and Δ_R^ρ are very sensitive with the changes of \tilde{m}_L and \tilde{m}_R . More details, Fig.4 draws the dependence of $|\Delta_R^\rho|^2/|\Delta_L^\rho|^2$ on $|\mu_\rho|/\tilde{m}_L$, where $m' = m_\chi = \tilde{m}_L \equiv m_{SUSY}$ and four different fixed values of \tilde{m}_R . The maximal and minimal values of the ratio $|\Delta_R^\rho|^2/|\Delta_L^\rho|^2$ on all the curves in Fig.4 have the same value at different values of $|\mu_\rho|/\tilde{m}_{SUSY}$. In the parameter region where the Higgs-mediated diagrams give dominated contribution to Δ s, the ratio $|\Delta_R^\rho|^2/|\Delta_L^\rho|^2$ is very small ($< 10^{-3}$). But in the remaining parameters, that ratio is increased. In the limit $|\mu_\rho|/\tilde{m}_{SUSY} \geq 30$, the ratio $|\Delta_R^\rho|^2/|\Delta_L^\rho|^2$ reaches to constant value. More general, we can investigate the influence of \tilde{m}_R/\tilde{m}_L on the ratio $|\Delta_R^\rho|^2/|\Delta_L^\rho|^2$ through contour plots drawn in Fig.5. On the drawing results showed that $|\Delta_R^\rho|^2/|\Delta_L^\rho|^2 \leq \mathcal{O}(10^{-2})$ whenever $|\mu_\rho|/m_{SUSY} \leq 5$ and that ratio does not depend too much on the ratio \tilde{m}_R/\tilde{m}_L . However, in the limit $|\mu_\rho|/m_{SUSY} \geq 7$ and $\tilde{m}_R < 0.5\tilde{m}_L$, the ratio $|\Delta_R^\rho|^2/|\Delta_L^\rho|^2$ changes very rapidly if small changes \tilde{m}_L and \tilde{m}_R . It means that chirality effects of phenomena relating with Δ_L^ρ and Δ_R^ρ are sensitive with the change of ratio \tilde{m}_R/\tilde{m}_L at large values of μ_ρ . On the other hand, the left picture in Fig.5 indicates that when the ratio $|\mu_\rho|/m_{SUSY} \geq 7$, it will exist in some regions of parameter space of \tilde{m}_R, \tilde{m}_L at which the contributions of left and right-lepton sectors into the $H \rightarrow \mu\tau$ decay process are the same order. In this case, the pure gaugino-mediated diagrams give the dominated

contribution to both Δ_L^ρ and Δ_R^ρ , and also $\Delta_\mu^{2\rho}$ (see A.2 in Appendix A). Recalling that large values of $\Delta_\mu^{2\rho}$ can strongly affect directly on the ratio Y_μ/Y_τ . The results presented in Fig.5 again confirm that whenever $|\mu_\rho|/m_{SUSY} \geq 7$ and $\tilde{m}_R < 0.5\tilde{m}_L$, the right-lepton sector gives dominated contribution to the branching ratio of $H \rightarrow \mu\tau$ decay process.

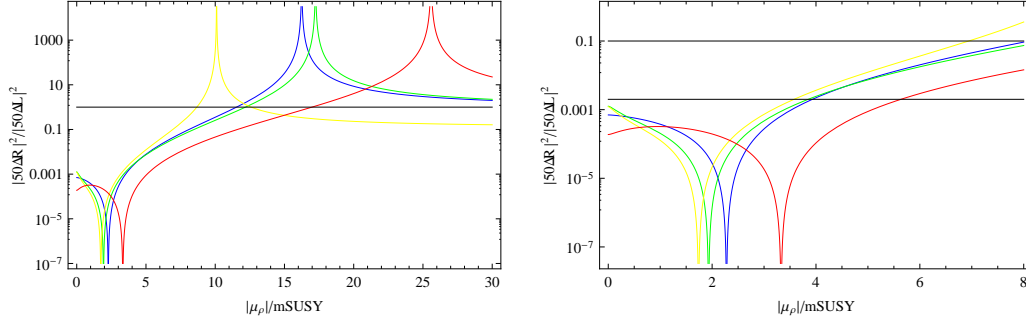


Fig. 4. $\frac{|\Delta_R^\rho|^2}{|\Delta_L^\rho|^2}$ as a function of $|\mu_\rho|/\tilde{m}_L$ with four different choices of masses ratios: 1) blue curve- $m' = \tilde{m}_R = \tilde{m}_L$; 2) green curve- $3m' = \tilde{m}_R = \tilde{m}_L$; 3) yellow curve- $m' = \tilde{m}_L = 3\tilde{m}_R$; 4) red curve- $m' = \tilde{m}_L = \tilde{m}_R/3$. A black line in the left-side of figure corresponds to the value $\frac{|\Delta_R^\rho|^2}{|\Delta_L^\rho|^2}$ equals 1. Both black lines in the right-side of figure are presented $\frac{|\Delta_R^\rho|^2}{|\Delta_L^\rho|^2}$ are 2.10^{-3} and 0.1.

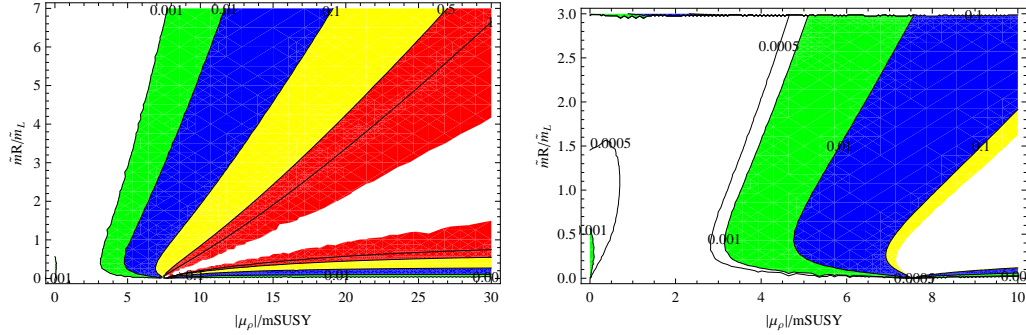


Fig. 5. Contour plot of $\frac{|\Delta_R^\rho|^2}{|\Delta_L^\rho|^2}$, \tilde{m}_R/\tilde{m}_L vs $|\mu_\rho|/m_{SUSY}$, where $\tilde{m}_R = \tilde{m}_{\nu_R}$, $m' = m_\lambda = \tilde{m}_L = \tilde{m}_{\nu_L} = m_{SUSY}$. The red region corresponds to the values of $\frac{|\Delta_R^\rho|^2}{|\Delta_L^\rho|^2} \geq 0.5$.

Now we investigate more details the region of parameter space where Higgsino-mediated diagrams give a dominated contribution. In this region of parameter space, both $\Delta_\mu^{2\rho}$ and Δ_R^ρ are much smaller than Δ_L^ρ so we just focus on Δ_L^ρ . From the Fig.6, we can estimate the ratio of $Br(H \rightarrow \mu\tau)/Br(H \rightarrow \tau\tau)$ that can reach to order of 10^{-3} in the limit $0.1 \leq |\mu_\rho|/M_{SUSY} \leq 6$ and $0.1 \leq |\tilde{m}_g|/M_{SUSY} \leq 7$ where \tilde{m}_g is mass of gauginos. Let us briefly review the decay properties of neutral Higgs bosons in the SUSYE331 model. At the tree level, the couplings of neutral Higgs bosons to up-fermions, down-fermion are modified with respect to the SM coupling by factors which are given in Table 1.

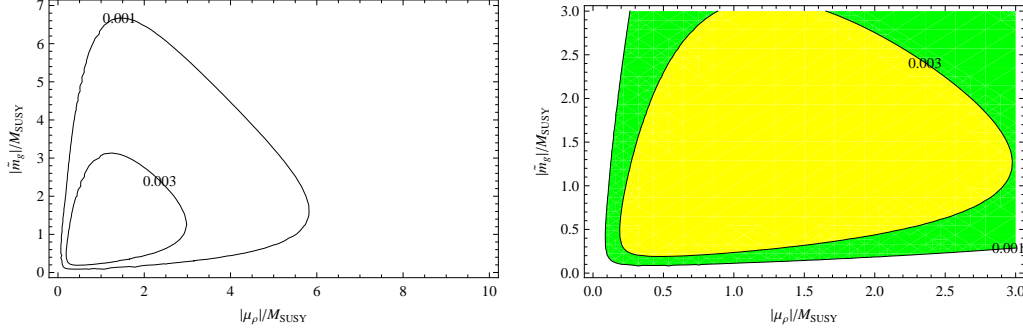


Fig. 6. Countour plot of $BR(H \rightarrow \mu\tau)/BR(H \rightarrow \tau\tau)$, \tilde{m}_g vs $|\mu_\rho|/m_{SUSY}$, where $m' = m_\lambda = \tilde{m}_g$ and $\tilde{m}_R = \tilde{m}_{\nu_R} = \tilde{m}_L = \tilde{m}_{\nu_L} = m_{SUSY}$. In the left picture, the green and yellow regions correspond to the values of $BR(H \rightarrow \mu\tau)/BR(H \rightarrow \tau\tau) \geq \mathcal{O}(10^{-3})$.

Table 1

Coupling of neutral Higgs bosons to fermion.

Particles	up-fermion	down-fermion	exotic up-quark	exotic down-quark
SM Higgs	1	1	0	0
φ_{Sa36}	c_α	c_α	s_α/s_γ	c_α/s_γ
ϕ_{Sa36}	s_α	s_α	c_α	s_α

We assume that all exotic quarks have masses heavier than that of all neutral Higgses. It means that the neutral Higgs cannot decay into the exotic quarks. The neutral Higgs bosons may decay mainly into the pairs of fermions. This prediction depends on the mass of the neutral Higgs. For neutral Higgs φ_{Sa36} , its mass depends on the vacuum expectation values v, v' . So it should be predicted SM Higgs with mass smaller than about 130 GeV. Decay of φ_{Sa36} to $b\bar{b}$ and $\tau\bar{\tau}$ are dominated, the branching ratios of 90 percents and 8 percents, respectively. Combined with the results in Fig.6, the branching ratio $Br(\varphi_{Sa36} \rightarrow \mu\tau)$ is 8×10^{-3} percents. This may be a good signification of new physics in the present limits of colliders. For neutral Higgs ϕ_{Sa36} , it is heavy Higgs, the main productions of decay are the gauge bosons such as W^+W^- , ZZ, \dots . Hence, the branching ratio $\phi \rightarrow \mu\tau$ is very suppressed. We would like to note that the effective interactions of the muon, tauon and Higgs given in (35) not only leads to the LFV of Higgs decay process, but also affects the other physical processes with flavor-lepton violations. Some of these processes which are looked seriously by present experiments are, for instance, $\tau \rightarrow \mu\mu\mu$ and $\tau \rightarrow \mu\gamma$. Let us apply the effective couplings given in (35) to the $\tau \rightarrow \mu\mu\mu$ decay process. In a general way-regardless of the model, the general effective Lagrangian describing decay of $\tau \rightarrow \mu\mu\mu$ was studied in [23]. However, in this work we focus on the effect of the Higgs-mediated LFV interactions on the $\tau \rightarrow \mu\mu\mu$ decay process. Hence, the four dimensional effective Lagrangian which is built through Higgs exchange is formulated by

$$\begin{aligned} \mathcal{L}_{\tau\mu\mu\mu}^{eff} = & -2\sqrt{2}G_F m_\mu m_\tau \tan\gamma \left(\frac{s_\alpha^2}{m_{\phi_{Sa36}}^2} + \frac{c_\alpha^2}{m_{\varphi_{Sa36}}^2} \right) (\mu^c \mu + \bar{\mu} \bar{\mu}^c) \\ & \times (\Delta_L^\rho \tau^c \mu + \Delta_R^\rho \mu^c \tau) + \text{H.c.} \end{aligned} \quad (43)$$

We would like to remind that the decay process of $\tau \rightarrow \mu\mu\mu$ were investigated, by [5,23] for examples, in a general model-independent way. The predicted results show that when Higgs exchange effects are much smaller than other ones, the ratio $Br(\tau \rightarrow 3\mu)/Br(\tau \rightarrow \mu\gamma)$ becomes constant with a value $\sim \mathcal{O}(10^{-3})$. Now, we will discuss in more details whether Higgs-mediated effects can be make any significations to the ratio $Br(\tau \rightarrow 3\mu)/Br(\tau \rightarrow \mu\gamma)$ in the SUSYE331 model. We can divide our results into two cases, namely ϕ_{Sa36}^* and φ_{Sa36}^* Higgs-mediated effects. The results can be written in two respective forms:

$$\begin{aligned} BR(\tau^- \rightarrow \mu^- \mu^+ \mu^-)_{\phi_{Sa36}^*} &= \frac{1}{8} \tan^2 \gamma \frac{m_\mu^2 m_\tau^2}{m_{\phi_{Sa36}}^4} s_\alpha^4 (|\Delta_L^\rho|^2 + |\Delta_R^\rho|^2) \\ &\simeq 7 \times 10^{-11} \left(\frac{\tan \gamma}{40} \right)^2 \left(\frac{100 \text{GeV}}{m_{\phi_{Sa36}}} \right)^4 \\ &\times \left(\frac{|\Delta_L^\rho|^2 + |\Delta_R^\rho|^2}{10^{-3}} \right) s_\alpha^4 \end{aligned} \quad (44)$$

and

$$\begin{aligned} BR(\tau^- \rightarrow \mu^- \mu^+ \mu^-)_{\varphi_{Sa36}^*} &= \frac{1}{8} \tan^2 \gamma \frac{m_\mu^2 m_\tau^2}{m_{\varphi_{Sa36}}^4} c_\alpha^4 (|\Delta_L^\rho|^2 + |\Delta_R^\rho|^2) \\ &\simeq 7 \times 10^{-11} \left(\frac{\tan \gamma}{40} \right)^2 \left(\frac{100 \text{GeV}}{m_{\varphi_{Sa36}}} \right)^4 \\ &\times \left(\frac{|\Delta_L^\rho|^2 + |\Delta_R^\rho|^2}{10^{-3}} \right) c_\alpha^4. \end{aligned} \quad (45)$$

These results immediately lead to a consequence: the maximum contribution of Higgs exchange processes can be estimated through the formula:

$$\begin{aligned} BR(\tau^- \rightarrow \mu^- \mu^+ \mu^-)_{H^*} &\simeq 7 \times 10^{-11} \left(\frac{\tan \gamma}{40} \right)^2 \left(\frac{100 \text{GeV}}{m_H} \right)^4 \\ &\times \left(\frac{|\Delta_L^\rho|^2 + |\Delta_R^\rho|^2}{10^{-3}} \right). \end{aligned} \quad (46)$$

The values of the branching ratios decrease rapidly corresponding to the enhancement of Higgs masses . We stress that in the model under consideration,

the $\phi_{S_{a36}}$ is identified with the SM Higgs boson and the remain, $\phi_{S_{a36}}$, is heavy one. Overall, in our model, the SM Higgs-mediated gives larger contribution to the branching ratio of the $\tau \rightarrow \mu\mu\mu$ decay process than that of heavy Higgs. That kind of branching increases if the $\tan\gamma$ increases. The branching ratio estimated in (46) is $\simeq 10^{-11}$ in the limit of $\tan\gamma \simeq 50$ and the Higgs mass is order of 100 GeV. However, the branching ratio of $\tau \rightarrow \mu\mu\mu$ can be reached to the present limits of experiment $BR(\tau^- \rightarrow \mu^- \mu^+ \mu^-) \leq 3.2 \times 10^{-8}$ [24]. It means that the contribution to $\tau \rightarrow \mu\mu\mu$ is suppressed in the limit of $\tan\gamma \simeq 50$. This result is different from that predicted in the MSSM model [8,4,5]. In particular, for the MSSM, the dominant contributions to $BR(\tau \rightarrow \mu\mu\mu)$ are induced by the dipole term and the Higgs-mediated term at the limit $\tan\beta = 50, m_A = 100$ GeV.

Because of sub-dominated contribution of Higgs-mediated to $BR(\tau \rightarrow \mu\mu\mu)$, the dominated contribution to that branching ratio is still obtained from the photon-penguin couplings. This result leads to the values of well-known ratios such as

$$\frac{Br(\tau \rightarrow 3\mu)}{BR(\tau \rightarrow \mu\gamma)} \simeq \mathcal{O}(10^{-3}) \quad (47)$$

The predicted result is the concerned result given in [8,5,23,25].

We emphasize that in the SUSYE331 model, in order to get the dominated contribution to the $B(\tau \rightarrow \mu\mu\mu)$, the values of $\tan\gamma$ must be 10^2 . In this limit of $\tan\gamma$, the result given in (47) is not holden.

5 Conclusions

In this paper, we have studied the LFV interactions of Higgs bosons in the SUSYE331 model. We have the unique existence of the lepton-number violation in the slepton sector at the tree level. On the basis of this assumption we have examined the lepton-number violating interactions of Higgs bosons at the one-loop level. Specially we have concentrated our study on the LFV couplings of Higgs bosons with muon and tauon. The analytical expressions of the effective Higgs-muon-tauon couplings are established at the one-loop level. One of the features is that the model does not contain the LFV interactions of neutral pseudo-scalar Higgs bosons. For the neutral Higgs scalars, the model contains two types of radiative interactions that violate lepton number, namely, $\phi_{S_{a36}}\mu\tau$ and $\varphi_{S_{a36}}\mu\tau$. These effective couplings depend on ratios of SUSY mass parameters and $\tan\gamma$. There is an exactly similar to the other SUSY models, all LFV couplings are built from two types of diagrams as Higgs-mediated diagrams and pure gaugino-mediated ones. Depending on the

SUSY parameters, each type of diagram gives the main contribution to LFV couplings. In this work, we have also studied the branching ratio of the neutral Higgs decay into muon and tauon. In the limit $|\mu_\rho|/m_{SUSY} \leq 7$, the ratio of $BR(H \rightarrow \tau\mu)/BR(H \rightarrow \tau\tau)$ in this region can reach to values that can be observed by near future experiments and the contribution from both left and right LFV sectors to $Br(H \rightarrow \mu\tau)$ are the same order. Outside this region the effects of left and right LFV terms mix in different ways in different regions of mass parameter space. We predicted that for the SM Higgs boson, LHC may detect the decay of SM Higgs boson to muon and tauon. For heavy Higgs bosons, the branching of LFV decay is very suppressed. We have also studied the contribution of Higgs exchange to decay $H \rightarrow 3\mu$. In the limit $\tan\gamma = 50$, the $Br(H \rightarrow 3\mu)$ is very small, out of direct detection of present searching of experiment and it leads to predicted results such as the ratio of $BR(\tau \rightarrow 3\mu)/BR(\tau \rightarrow \mu\gamma)$.

Acknowledgments

L. T. H would like to thank the Organizers of KEK-Vietnam visiting Program 2011 (Exchange Program for East Asia Young Researchers, JSPS), especially Prof. Y. Kurihara, for the support for his initial work at KEK. This work was supported in part by the National Foundation for Science and Technology Development (NAFOSTED) of Vietnam under Grant No. 103.01-2011.63.

A Analytic formulas and diagrams contributing to Δ s

Let us write down all expressions of Δ s given as following

$$\begin{aligned} \Delta_\mu^{1\rho} = & -\frac{g'^2}{108\pi^2}\mu_\rho m' \left[c_L^2 I_3(m'^2, \mu_\rho^2, \tilde{m}_{L_2}^2) + s_L^2 I_3(m'^2, \mu_\rho^2, \tilde{m}_{L_3}^2) \right] \\ & -\frac{g^2}{24\pi^2}\mu_\rho m_\lambda \left[c_L^2 I_3(m_\lambda^2, \mu_\rho^2, \tilde{m}_{L_2}^2) + s_L^2 I_3(m_\lambda^2, \mu_\rho^2, \tilde{m}_{L_3}^2) \right] \\ & -\frac{g^2}{16\pi^2}\mu_\rho m_\lambda \left[c_{\nu_L}^2 I_3(m_\lambda^2, \mu_\rho^2, \tilde{m}_{\nu_{L_2}}^2) + s_{\nu_L}^2 I_3(m_\lambda^2, \mu_\rho^2, \tilde{m}_{\nu_{L_3}}^2) \right] \\ & -\frac{g^2}{16\pi^2}\mu_\rho m_\lambda \left[c_{\nu_R}^2 I_3(m_\lambda^2, \mu_\rho^2, \tilde{m}_{\nu_{R_2}}^2) + s_{\nu_R}^2 I_3(m_\lambda^2, \mu_\rho^2, \tilde{m}_{\nu_{R_3}}^2) \right] \\ & + \frac{Y_{\nu\mu\tau}(h_{\mu\tau} - h_{\tau\mu})\mu_\rho}{8\pi^2} \\ & \times \left[s_{\nu_{(L-R)}}^2 \left(I_3(\mu_\rho^2, \tilde{m}_{\nu_{L_2}}^2, \tilde{m}_{\nu_{R_2}}^2) + I_3(\mu_\rho^2, \tilde{m}_{\nu_{L_3}}^2, \tilde{m}_{\nu_{R_3}}^2) \right) \right] \end{aligned}$$

$$\begin{aligned}
& + c_{\nu(L-R)}^2 \left(I_3(\mu_\rho^2, \tilde{m}_{\nu_{L3}}^2, \tilde{m}_{\nu_{R2}}^2) + I_3(\mu_\rho^2, \tilde{m}_{\nu_{L2}}^2, \tilde{m}_{\nu_{R3}}^2) \right) \\
& + \frac{g'^2}{288\pi^2} \mu_\rho m' \left[c_L^2 \left(c_R^2 I_3(m'^2, \tilde{m}_{L2}^2, \tilde{m}_{R2}^2) + s_R^2 I_3(m'^2, \tilde{m}_{L2}^2, \tilde{m}_{R3}^2) \right) \right. \\
& \left. + s_L^2 \left(c_R^2 I_3(m'^2, \tilde{m}_{L3}^2, \tilde{m}_{R2}^2) + s_R^2 I_3(m'^2, \tilde{m}_{L3}^2, \tilde{m}_{R3}^2) \right) \right]. \tag{A.1}
\end{aligned}$$

$$\begin{aligned}
\Delta_\mu^{2\rho} &= \frac{g'^2}{288\pi^2} \mu_\rho m' s_L c_L s_R c_R \left[I_3(m'^2, \tilde{m}_{L2}^2, \tilde{m}_{R2}^2) - I_3(m'^2, \tilde{m}_{L2}^2, \tilde{m}_{R3}^2) \right. \\
& \left. - I_3(m'^2, \tilde{m}_{L3}^2, \tilde{m}_{R2}^2) + I_3(m'^2, \tilde{m}_{L3}^2, \tilde{m}_{R3}^2) \right]. \tag{A.2}
\end{aligned}$$

$$\begin{aligned}
\Delta_\tau^\rho &= -\frac{g'^2}{108\pi^2} \mu_\rho m' \left[s_L^2 I_3(m'^2, \mu_\rho^2, \tilde{m}_{L2}^2) + c_L^2 I_3(m'^2, \mu_\rho^2, \tilde{m}_{L3}^2) \right] \\
& - \frac{g^2}{24\pi^2} \mu_\rho m_\lambda \left[s_L^2 I_3(m_\lambda^2, \mu_\rho^2, \tilde{m}_{L2}^2) + c_L^2 I_3(m_\lambda^2, \mu_\rho^2, \tilde{m}_{L3}^2) \right] \\
& - \frac{g^2}{16\pi^2} \mu_\rho m_\lambda \left[s_{\nu_L}^2 I_3(m_\lambda^2, \mu_\rho^2, \tilde{m}_{\nu_{L2}}^2) + c_{\nu_L}^2 I_3(m_\lambda^2, \mu_\rho^2, \tilde{m}_{\nu_{L3}}^2) \right] \\
& - \frac{g^2}{16\pi^2} \mu_\rho m_\lambda \left[s_{\nu_R}^2 I_3(m_\lambda^2, \mu_\rho^2, \tilde{m}_{\nu_{R2}}^2) + c_{\nu_R}^2 I_3(m_\lambda^2, \mu_\rho^2, \tilde{m}_{\nu_{R3}}^2) \right] \\
& + \frac{Y_{\nu\mu\tau}(h_{\mu\tau} - h_{\tau\mu})\mu_\rho}{8\pi^2} \\
& \times \left[s_{\nu(L-R)}^2 \left(I_3(\mu_\rho^2, \tilde{m}_{\nu_{L2}}^2, \tilde{m}_{\nu_{R2}}^2) + I_3(\mu_\rho^2, \tilde{m}_{\nu_{L3}}^2, \tilde{m}_{\nu_{R3}}^2) \right) \right. \\
& \left. + c_{\nu(L-R)}^2 \left(I_3(\mu_\rho^2, \tilde{m}_{\nu_{3L}}^2, \tilde{m}_{\nu_{R2}}^2) + I_3(\mu_\rho^2, \tilde{m}_{\nu_{L2}}^2, \tilde{m}_{\nu_{R3}}^2) \right) \right] \\
& + \frac{g'^2}{288\pi^2} \mu_\rho m' \left[s_L^2 \left(s_R^2 I_3(m'^2, \tilde{m}_{L2}^2, \tilde{m}_{R2}^2) + c_R^2 I_3(m'^2, \tilde{m}_{L2}^2, \tilde{m}_{R3}^2) \right) \right. \\
& \left. + c_L^2 \left(s_R^2 I_3(m'^2, \tilde{m}_{L3}^2, \tilde{m}_{R2}^2) + c_R^2 I_3(m'^2, \tilde{m}_{L3}^2, \tilde{m}_{R3}^2) \right) \right]. \tag{A.3}
\end{aligned}$$

$$\begin{aligned}
\Delta_\mu^{1\rho'} &= \frac{Y_{\nu\mu\tau}^2}{4\pi^2} \mu_\rho^2 \left[s_{\nu(L-R)}^2 \left(I_3(\mu_\rho^2, \tilde{m}_{\nu_{L2}}^2, \tilde{m}_{\nu_{R2}}^2) + I_3(\mu_\rho^2, \tilde{m}_{\nu_{L3}}^2, \tilde{m}_{\nu_{R3}}^2) \right) \right. \\
& \left. + c_{\nu(L-R)}^2 \left(I_3(\mu_\rho^2, \tilde{m}_{\nu_{L2}}^2, \tilde{m}_{\nu_{R3}}^2) + I_3(\mu_\rho^2, \tilde{m}_{\nu_{L3}}^2, \tilde{m}_{\nu_{R2}}^2) \right) \right]. \tag{A.4}
\end{aligned}$$

$$\begin{aligned}
\Delta_\mu^{2\rho'} &= \frac{g'^2 m'}{144\pi^2} \\
& \times \left[\frac{h'_\mu c_L c_R + h'_\tau s_L s_R + h'_{\mu\tau} c_L s_R + h'_{\tau\mu} s_L c_R}{Y_\tau} c_L c_R I_3(m'^2, \tilde{m}_{L2}^2, \tilde{m}_{R2}^2) \right. \\
& \left. + \frac{h'_\mu s_L s_R + h'_\tau c_L c_R - h'_{\mu\tau} s_L c_R - h'_{\tau\mu} c_L s_R}{Y_\tau} s_L s_R I_3(m'^2, \tilde{m}_{L3}^2, \tilde{m}_{R3}^2) \right]
\end{aligned}$$

$$\begin{aligned}
& - \frac{-h'_\mu s_{LCR} + h'_\tau c_{LSR} - h'_{\mu\tau} s_{LSR} + h'_{\tau\mu} c_{LCR}}{Y_\tau} s_{LCR} I_3(m'^2, \tilde{m}_{L_3}^2, \tilde{m}_{R_2}^2) \\
& - \frac{-h'_\mu c_{LSR} + h'_\tau s_{LCR} + h'_{\mu\tau} c_{LCR} - h'_{\tau\mu} s_{LSR}}{Y_\tau} c_{LSR} I_3(m'^2, \tilde{m}_{L_2}^2, \tilde{m}_{R_3}^2) \Big].
\end{aligned} \tag{A.5}$$

$$\begin{aligned}
\Delta_\tau^{\rho'} &= \Delta_\mu^{1\rho'} + \frac{g'^2 m'}{144\pi^2} \\
& \times \left[\frac{h'_\mu c_{LCR} + h'_\tau s_{LSR} + h'_{\mu\tau} c_{LSR} + h'_{\tau\mu} s_{LCR}}{Y_\tau} s_{LSR} I_3(m'^2, \tilde{m}_{L_2}^2, \tilde{m}_{R_2}^2) \right. \\
& + \frac{h'_\mu s_{LSR} + h'_\tau c_{LCR} - h'_{\mu\tau} s_{LCR} - h'_{\tau\mu} c_{LSR}}{Y_\tau} c_{LCR} I_3(m'^2, \tilde{m}_{L_3}^2, \tilde{m}_{R_3}^2) \\
& + \frac{-h'_\mu s_{LCR} + h'_\tau c_{LSR} - h'_{\mu\tau} s_{LSR} + h'_{\tau\mu} c_{LCR}}{Y_\tau} c_{LSR} I_3(m'^2, \tilde{m}_{L_3}^2, \tilde{m}_{R_2}^2) \\
& \left. + \frac{-h'_\mu c_{LSR} + h'_\tau s_{LCR} + h'_{\mu\tau} c_{LCR} - h'_{\tau\mu} s_{LSR}}{Y_\tau} s_{LCR} I_3(m'^2, \tilde{m}_{L_2}^2, \tilde{m}_{R_3}^2) \right]
\end{aligned} \tag{A.6}$$

In the case of $\Delta_L^{\rho'}$, it also receives contributions from two diagrams (similar to diagrams *e* and *f* in Fig.1) which cancel each other. Therefore we do not repeat them in Fig.A.4. Formula of $\Delta_L^{\rho'}$ then is

$$\begin{aligned}
\Delta_L^{\rho'} &= \frac{g'^2 m'}{144\pi^2} \\
& \times \left[\frac{h'_\mu c_{LCR} + h'_\tau s_{LSR} + h'_{\mu\tau} c_{LSR} + h'_{\tau\mu} s_{LCR}}{Y_\tau} c_{LSR} I_3(m'^2, \tilde{m}_{L_2}^2, \tilde{m}_{R_2}^2) \right. \\
& - \frac{h'_\mu s_{LSR} + h'_\tau c_{LCR} - h'_{\mu\tau} s_{LCR} - h'_{\tau\mu} c_{LSR}}{Y_\tau} s_{LCR} I_3(m'^2, \tilde{m}_{L_3}^2, \tilde{m}_{R_3}^2) \\
& - \frac{-h'_\mu s_{LCR} + h'_\tau c_{LSR} - h'_{\mu\tau} s_{LSR} + h'_{\tau\mu} c_{LCR}}{Y_\tau} s_{LSR} I_3(m'^2, \tilde{m}_{L_3}^2, \tilde{m}_{R_2}^2) \\
& \left. + \frac{-h'_\mu c_{LSR} + h'_\tau s_{LCR} + h'_{\mu\tau} c_{LCR} - h'_{\tau\mu} s_{LSR}}{Y_\tau} c_{LCR} I_3(m'^2, \tilde{m}_{L_2}^2, \tilde{m}_{R_3}^2) \right].
\end{aligned} \tag{A.7}$$

$$\begin{aligned}
\Delta_R^{\rho'} &= \frac{g'^2 m'}{144\pi^2} \\
& \times \left[\frac{h'_\mu c_{LCR} + h'_\tau s_{LSR} + h'_{\mu\tau} c_{LSR} + h'_{\tau\mu} s_{LCR}}{Y_\tau} s_{LCR} I_3(m'^2, \tilde{m}_{L_2}^2, \tilde{m}_{R_2}^2) \right.
\end{aligned}$$

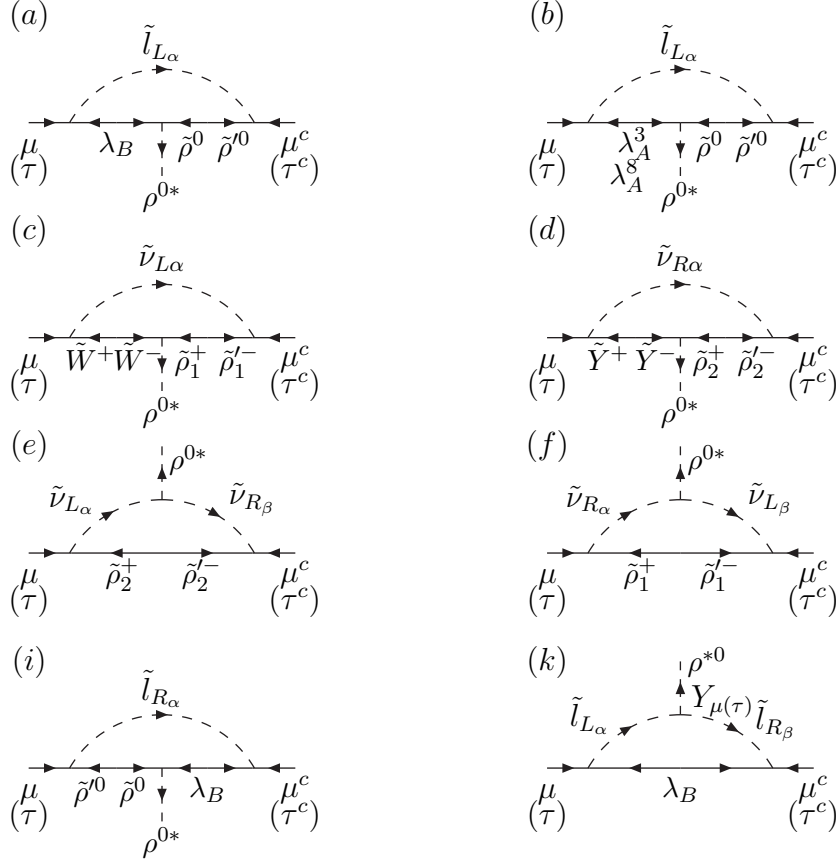


Fig. A.1. Diagrams contributing to $\Delta_\mu^{1\rho}$ (or Δ_τ^ρ).

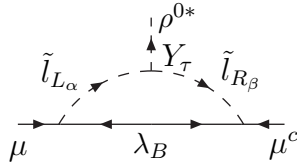


Fig. A.2. Diagram contributing to $\Delta_\mu^{2\rho}$.

$$\begin{aligned}
& - \frac{h'_\mu s_{LSR} + h'_\tau c_{LCR} - h'_{\mu\tau} s_{LCR} - h'_{\tau\mu} c_{LSR}}{Y_\tau} c_{LSR} I_3(m'^2, \tilde{m}_{L_3}^2, \tilde{m}_{R_3}^2) \\
& + \frac{-h'_\mu s_{LCR} + h'_\tau c_{LSR} - h'_{\mu\tau} s_{LSR} + h'_{\tau\mu} c_{LCR}}{Y_\tau} c_{LCR} I_3(m'^2, \tilde{m}_{L_3}^2, \tilde{m}_{R_2}^2) \\
& - \frac{-h'_\mu c_{LSR} + h'_\tau s_{LCR} + h'_{\mu\tau} c_{LCR} - h'_{\tau\mu} s_{LSR}}{Y_\tau} s_{LSR} I_3(m'^2, \tilde{m}_{L_2}^2, \tilde{m}_{R_3}^2) \Big].
\end{aligned} \tag{A.8}$$

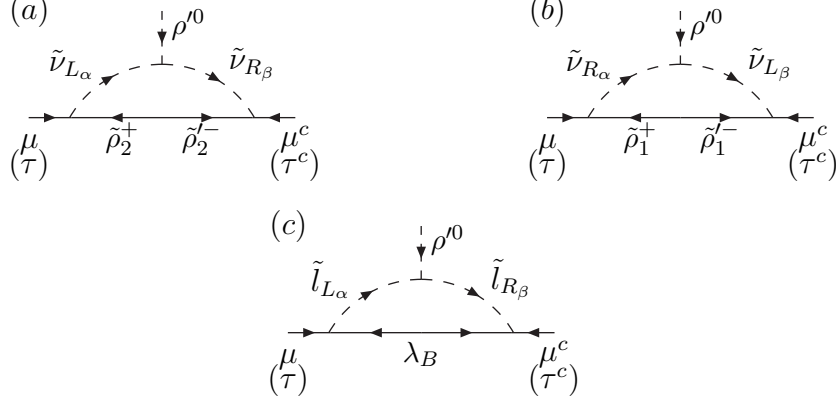


Fig. A.3. Diagrams contributing to $\Delta_\mu^{1\rho'}$ [(a), (b)], $\Delta_\mu^{2\rho'}$ [(c)] (or $\Delta_\tau^{\rho'}$ [(a), (b), (c)]).



Fig. A.4. Diagrams contributing to $\Delta_L^{\rho'}$ [(a)] and $\Delta_R^{\rho'}$ [(b)].

B Lagrangian

We have denoted that $f_{L,R}(\bar{f}_{L,R}^c)$ are two component spinor of the generic matter left-handed and right-handed fermion, respectively. The $\tilde{f}_L(\tilde{f}_L^c)$ are their superpartners which satisfy $(\tilde{f}_L^c = (f_R)^\dagger T, \tilde{f}_L^c = \tilde{f}_R^*)$. The four-component Dirac spinor can be represented through two-component spinor such as: $\mu \equiv (\mu_L, \mu_R) = (\mu_L, \bar{\mu}_L^c)$ and $\tilde{\mu} \equiv (\tilde{\mu}_L, \tilde{\mu}_R) = (\tilde{\mu}_L, \tilde{\mu}_L^{c*})$. We also emphasize that three left handed leptons contained in the triplet L_{aL} of $SU(3)_L$ are $(f_{a1L}, f_{a2L}, f_{a3L})$:

$$\begin{aligned} f_{a1L} &\in \{\nu_{eL}, \nu_{\mu L}, \nu_{\tau L}\} \equiv \{\nu_{1L}, \nu_{2L}, \nu_{3L}\}, \\ f_{a2L} &\in \{e_L, \mu_L, \tau_L\}, \\ f_{a3L} &\in \{\nu_{eL}^c, \nu_{\mu L}^c, \nu_{\tau L}^c\} \equiv \{\nu_{1L}^c, \nu_{2L}^c, \nu_{3L}^c\} \equiv \{(\nu_1^c)_L, (\nu_2^c)_L, (\nu_3^c)_L\} \end{aligned} \quad (\text{B.1})$$

while f_{aL}^c is singlet under $SU(3)_L$. Conventions for two component spinors used in our paper are the same as those given in [5] except the lower index L , which is used to distinguish between Dirac spinors f and left-handed Weyl spinors f_L .

Next, let us find the interactional vertices relating with our calculation. We start to collect related terms from the Lagrangian given in [15,26] into the following ones:

(1) Gaugino and Higgsino mass terms

$$\begin{aligned}
\mathcal{L}_{gh} &= - \left[\frac{1}{2} m_\lambda \sum_{b=1}^8 (\lambda_A^b \lambda_A^b) + \frac{1}{2} m' \lambda_B \lambda_B + \mu_\chi \tilde{\chi} \tilde{\chi}' + \mu_\rho \tilde{\rho} \tilde{\rho}' \right] + \text{H.c} \\
&= - \frac{1}{2} m' \lambda_B \lambda_B - m_\lambda \tilde{W}^+ \tilde{W}^- - \frac{1}{2} m_\lambda \lambda_A^3 \lambda_A^3 \\
&\quad - m_\lambda \tilde{Y}'^+ \tilde{Y}'^- - m_\lambda \tilde{X}^{0*} \tilde{X}^0 - \frac{1}{2} m_\lambda \lambda_A^8 \lambda_A^8 - \mu_\chi (\tilde{\chi}_1^0 \tilde{\chi}_1'^0 + \tilde{\chi}^- \tilde{\chi}'^+ + \tilde{\chi}_2^0 \tilde{\chi}_2'^0) \\
&\quad - \mu_\rho (\tilde{\rho}_1^+ \tilde{\rho}_1'^- + \tilde{\rho}^0 \tilde{\rho}'^0 + \tilde{\rho}_2^+ \tilde{\rho}_2'^-) + \text{H.c.}
\end{aligned} \tag{B.2}$$

where

$$\begin{aligned}
\tilde{W}^\pm &\equiv \frac{1}{\sqrt{2}} (\lambda_A^1 \mp i \lambda_A^2); & \tilde{Y}^\pm &\equiv \frac{1}{\sqrt{2}} (\lambda_A^6 \pm i \lambda_A^7), \\
\tilde{X} &\equiv \frac{1}{\sqrt{2}} (\lambda_A^4 + i \lambda_A^5); & \tilde{X}^* &\equiv \frac{1}{\sqrt{2}} (\lambda_A^4 - i \lambda_A^5)
\end{aligned} \tag{B.3}$$

where we have used the results of mass eigenstate states for Higgsinos and gauginos given in [16] and [18].

(2) Fermion-sfermion-gaugino interaction terms:

$$\begin{aligned}
\mathcal{L}_{\tilde{l}\tilde{W}} &= - \frac{ig'}{\sqrt{3}} \left[-\frac{1}{3} (\bar{\tilde{L}} \tilde{L} \bar{\lambda}_B - \tilde{L}^\dagger L \lambda_B) + (\bar{\tilde{l}}^c \tilde{l}^c \bar{\lambda}_B - \tilde{l}^{c*} l^c \lambda_B) \right] \\
&\quad - \frac{ig}{\sqrt{2}} (\bar{\tilde{L}} \lambda^i \tilde{L} \bar{\lambda}_A^i - \tilde{L}^\dagger \lambda^i L \lambda_A^i),
\end{aligned} \tag{B.4}$$

where $i = 1, 2, \dots, 8$ is a color index and $L \equiv (L_{1L}, L_{2L}, L_{3L})^T$, $\tilde{L} \equiv (\tilde{L}_{1L}, \tilde{L}_{2L}, \tilde{L}_{3L})^T$, $\bar{l}^c = (l_{1R}, l_{2R}, l_{3R})^T \equiv (\bar{l}_{1L}^c, \bar{l}_{2L}^c, \bar{l}_{3L}^c)^T \equiv (e_R, \mu_R, \tau_R)^T \equiv (\bar{e}_L^c, \bar{\mu}_L^c, \bar{\tau}_L^c)^T$, and $\tilde{l}^c = (\tilde{l}_{1R}^*, \tilde{l}_{2R}^*, \tilde{l}_{3R}^*)^T \equiv (\tilde{e}_R^*, \tilde{\mu}_R^*, \tilde{\tau}_R^*)^T$. In this paper we just focus on interactions relating with two fermions, namely $l_{aL} = \{\mu_L, \tau_L\}$. All interested terms are given as

$$\begin{aligned}
\mathcal{L}_{\tilde{l}\tilde{W}} &= \left[\bar{\mu}_L \left(\frac{ig'}{3\sqrt{3}} \bar{\lambda}_B + \frac{ig}{\sqrt{2}} (\bar{\lambda}_A^3 - \frac{1}{\sqrt{3}} \bar{\lambda}_A^8) \right) \tilde{\mu}_L \right. \\
&\quad - \mu_L \left(\frac{ig'}{3\sqrt{3}} \lambda_B + \frac{ig}{\sqrt{2}} (\lambda_A^3 - \frac{1}{\sqrt{3}} \lambda_A^8) \right) \tilde{\mu}_L^* \\
&\quad - \frac{ig'}{\sqrt{3}} (\bar{\mu}_L^c \tilde{\mu}_L^c \bar{\lambda}_B - \mu_L^c \tilde{\mu}_L^{c*} \lambda_B) + \frac{ig}{\sqrt{2}} (\bar{\mu}_L \tilde{\mu}_L \bar{\lambda}_A^3 - \tilde{\mu}_L^* \mu_L \lambda_A^3) \\
&\quad + \frac{ig}{\sqrt{2}} (\bar{\mu}_L \tilde{\mu}_L \bar{\lambda}_A^8 - \tilde{\mu}_L^* \mu_L \lambda_A^8) \\
&\quad \left. - ig \left((\bar{\mu}_L \tilde{W}^+ \tilde{\nu}_{\mu L} - \mu_L \tilde{W}^+ \tilde{\nu}_{\mu L}^*) + (\bar{\mu}_L \tilde{Y}^+ \tilde{\nu}_{\mu L}^c - \mu_L \tilde{Y}^+ \tilde{\nu}_{\mu L}^{c*}) \right) \right] \\
&\quad + [\mu \rightarrow \tau].
\end{aligned} \tag{B.5}$$

From this, we list the related vertices in Table B.1

Vertex	factor	Vertex	factor
$\bar{\mu}_L \bar{\lambda}_B \tilde{\mu}_L$	$-\frac{g'}{3\sqrt{3}}$	$\mu_L \lambda_B \tilde{\mu}_L^*$	$\frac{g'}{3\sqrt{3}}$
$\bar{\mu}_L^c \tilde{\mu}_L^c \bar{\lambda}_B$	$\frac{g'}{\sqrt{3}}$	$\mu_L^c \tilde{\mu}_L^{c*} \lambda_B$	$\frac{-g'}{\sqrt{3}}$
$\bar{\mu}_L \tilde{\mu}_L \bar{\lambda}_A^3$	$\frac{-g}{\sqrt{2}}$	$\tilde{\mu}_L^* \mu_L \lambda_A^3$	$\frac{g}{\sqrt{2}}$
$\bar{\mu}_L \tilde{\mu}_L \bar{\lambda}_A^8$	$\frac{g}{\sqrt{6}}$	$\tilde{\mu}_L^* \mu_L \lambda_A^8$	$\frac{-g}{\sqrt{6}}$
$\bar{\mu}_L \tilde{W}^+ \tilde{\nu}_{\mu L}$	g	$\mu_L \tilde{W}^+ \tilde{\nu}_{\mu L}^*$	$-g$
$\bar{\mu}_L \tilde{Y}^+ \tilde{\nu}_{\mu L}^c$	g	$\mu_L \tilde{Y}^+ \tilde{\nu}_{\mu L}^{c*}$	$-g$
$\bar{\tau}_L \bar{\lambda}_B \tilde{\tau}_L$	$-\frac{g'}{3\sqrt{3}}$	$\tau_L \lambda_B \tilde{\tau}_L^*$	$\frac{g'}{3\sqrt{3}}$
$\bar{\tau}_L^c \tilde{\tau}_L^c \bar{\lambda}_B$	$\frac{g'}{\sqrt{3}}$	$\tau_L^c \tilde{\tau}_L^{c*} \lambda_B$	$\frac{-g'}{\sqrt{3}}$
$\bar{\tau}_L \tilde{\tau}_L \bar{\lambda}_A^3$	$\frac{-g}{\sqrt{2}}$	$\tilde{\tau}_L^* \tau_L \lambda_A^3$	$\frac{g}{\sqrt{2}}$
$\bar{\tau}_L \tilde{\tau}_L \bar{\lambda}_A^8$	$\frac{g}{\sqrt{6}}$	$\tilde{\tau}_L^* \tau_L \lambda_A^8$	$\frac{g}{-\sqrt{6}}$
$\bar{\tau}_L \tilde{W}^+ \tilde{\nu}_{\tau L}$	g	$\tau_L \tilde{W}^+ \tilde{\nu}_{\tau L}^*$	$-g$
$\bar{\tau}_L \tilde{Y}^+ \tilde{\nu}_{\tau L}^c$	g	$\tau_L \tilde{Y}^+ \tilde{\nu}_{\tau L}^{c*}$	$-g$

Table B.1

Vertices of lepton-slepton-gaussino interaction at tree level

(3) Higgs-Higgsino-gaugino:

$$\begin{aligned}
\mathcal{L}_{H\tilde{H}\tilde{V}} = & -\frac{ig'}{\sqrt{3}} \left[-\frac{1}{3}(\tilde{\chi}\chi\bar{\lambda}_B - \chi^\dagger\tilde{\chi}\lambda_B) + \frac{1}{3}(\tilde{\chi}'\chi'\bar{\lambda}_B - \chi'^\dagger\tilde{\chi}'\lambda_B) \right. \\
& + \frac{2}{3}(\tilde{\rho}\rho\bar{\lambda}_B - \rho^\dagger\tilde{\rho}\lambda_B) - \frac{2}{3}(\tilde{\rho}'\rho'\bar{\lambda}_B - \rho'^\dagger\tilde{\rho}'\lambda_B) \Big] \\
& - \frac{ig}{\sqrt{2}} \left[\tilde{\rho}\lambda^a\rho\bar{\lambda}_A^a - \rho^\dagger\lambda^a\tilde{\rho}\lambda_A^a + \tilde{\chi}\lambda^a\chi\bar{\lambda}_A^a - \chi^\dagger\lambda^a\tilde{\chi}\lambda_A^a \right. \\
& \left. - \tilde{\rho}'\lambda'^a\rho'\bar{\lambda}_A^a + \rho'^\dagger\lambda'^a\tilde{\rho}'\lambda_A^a - \tilde{\chi}'\lambda'^a\chi'\bar{\lambda}_A^a + \chi'^\dagger\lambda'^a\tilde{\chi}'\lambda_A^a \right] \quad (B.6)
\end{aligned}$$

Vertices of neutral Higgs-Higgsino-gaugino interactions are shown in table B.2

(4) **Yukawa interaction terms:**

$$\mathcal{L}_{\tilde{U}\tilde{H}} = -\frac{\lambda_{1ab}}{3} \left(L_{aL} \tilde{\rho}' \tilde{l}_{bL}^c + \tilde{L}_{aL} \tilde{\rho}' l_{bL}^c \right) - \frac{\lambda_{3ab}}{3} \left(L_{aL} \tilde{\rho} \tilde{L}_{bL} + \tilde{L}_{aL} \tilde{\rho} L_{bL} \right); \quad (B.7)$$

$$\mathcal{L}_{\tilde{U}H} = -\frac{\lambda_{1ab}}{3} L_{aL} l_{bL}^c \rho' - \frac{\lambda_{3ab}}{3} \epsilon^{\alpha\beta\gamma} (L_{aL})_\alpha (L_{bL})_\beta (\rho)_\gamma + \text{H.c.} \quad (B.8)$$

Our work needs only terms which include leptons μ or τ , such as:

$$\mathcal{L}_{\tilde{U}\tilde{H}} = -\frac{\lambda_{1ab}}{3} \left[l_{aL} \tilde{\rho}'^0 \tilde{l}_{bL}^c + (\tilde{\nu}_{aL} \tilde{\rho}'_1^- + \tilde{l}_{aL} \tilde{\rho}'^0 + \tilde{\nu}_{aL}^c \tilde{\rho}'_2^-) l_{bL}^c \right]$$

Table B.2

Vertices of the neutral Higgs-Higgsino-Gausino interactions

Vertex	Factor	Vertex	Factor
$\tilde{\chi}_1^0 \chi_1^0 \bar{\lambda}_B$	$\frac{-g'}{3\sqrt{3}}$	$\tilde{\chi}_1^0 \chi_1^{0\dagger} \lambda_B$	$\frac{g'}{3\sqrt{3}}$
$\tilde{\chi}_2^0 \chi_2^0 \bar{\lambda}_B$	$\frac{-g'}{3\sqrt{3}}$	$\tilde{\chi}_2^0 \chi_2^{0\dagger} \lambda_B$	$\frac{g'}{3\sqrt{3}}$
$\tilde{\chi}_1^0 \chi_1^0 \bar{\lambda}_A^3$	$\frac{g}{\sqrt{2}}$	$\tilde{\chi}_1^0 \chi_1^{0\dagger} \lambda_A^3$	$\frac{-g}{\sqrt{2}}$
$\tilde{\chi}_1^0 \chi_1^0 \bar{\lambda}_A^8$	$\frac{g}{\sqrt{6}}$	$\tilde{\chi}_1^0 \chi_1^{0\dagger} \lambda_A^8$	$\frac{-g}{\sqrt{6}}$
$\tilde{\chi}_2^0 \chi_2^0 \bar{\lambda}_A^8$	$\frac{-g\sqrt{2}}{\sqrt{3}}$	$\tilde{\chi}_2^0 \chi_2^{0\dagger} \lambda_A^8$	$\frac{g\sqrt{2}}{\sqrt{3}}$
$\tilde{\chi}_1'^0 \chi_1'^0 \bar{\lambda}_B$	$\frac{g'}{3\sqrt{3}}$	$\tilde{\chi}_1'^0 \chi_1'^{0\dagger} \lambda_B$	$\frac{-g'}{3\sqrt{3}}$
$\tilde{\chi}_2'^0 \chi_2'^0 \bar{\lambda}_B$	$\frac{g'}{3\sqrt{3}}$	$\tilde{\chi}_2'^0 \chi_2'^{0\dagger} \lambda_B$	$\frac{-g'}{3\sqrt{3}}$
$\tilde{\chi}_1'^0 \chi_1'^0 \bar{\lambda}_A^3$	$\frac{-g}{\sqrt{2}}$	$\tilde{\chi}_1'^0 \chi_1'^{0\dagger} \lambda_A^3$	$\frac{g}{\sqrt{2}}$
$\tilde{\chi}_1'^0 \chi_1'^0 \bar{\lambda}_A^8$	$\frac{-g}{\sqrt{6}}$	$\tilde{\chi}_1'^0 \chi_1'^{0\dagger} \lambda_A^8$	$\frac{g}{\sqrt{6}}$
$\tilde{\chi}_2'^0 \chi_2'^0 \bar{\lambda}_A^8$	$\frac{g\sqrt{2}}{\sqrt{3}}$	$\tilde{\chi}_2'^0 \chi_2'^{0\dagger} \lambda_A^8$	$\frac{-g\sqrt{2}}{\sqrt{3}}$
$\tilde{\rho}^0 \rho^0 \bar{\lambda}_B$	$\frac{2g'}{3\sqrt{3}}$	$\tilde{\rho}^0 \rho^{0\dagger} \lambda_B$	$\frac{-2g'}{3\sqrt{3}}$
$\tilde{\rho}^0 \rho^0 \bar{\lambda}_A^3$	$\frac{-g}{\sqrt{2}}$	$\tilde{\rho}^0 \rho^{0\dagger} \lambda_A^3$	$\frac{g}{\sqrt{2}}$
$\tilde{\rho}^0 \rho^0 \bar{\lambda}_A^8$	$\frac{g}{\sqrt{6}}$	$\tilde{\rho}^0 \rho^{0\dagger} \lambda_A^8$	$\frac{-g}{\sqrt{6}}$
$\tilde{\rho}'^0 \rho'^0 \bar{\lambda}_B$	$\frac{-2g'}{3\sqrt{3}}$	$\tilde{\rho}'^0 \rho'^{0\dagger} \lambda_B$	$\frac{2g'}{3\sqrt{3}}$
$\tilde{\rho}'^0 \rho'^0 \bar{\lambda}_A^3$	$\frac{g}{\sqrt{2}}$	$\tilde{\rho}'^0 \rho'^{0\dagger} \lambda_A^3$	$\frac{-g}{\sqrt{2}}$
$\tilde{\rho}'^0 \rho'^0 \bar{\lambda}_A^8$	$\frac{-g}{\sqrt{6}}$	$\tilde{\rho}'^0 \rho'^{0\dagger} \lambda_A^8$	$\frac{g}{\sqrt{6}}$
$\tilde{\chi}^- \tilde{W}^+ \chi_1^0$	g	$\chi^{0*} \tilde{W}^+ \tilde{\chi}^-$	$-g$
$\tilde{\chi}^- \tilde{Y}^+ \chi_2^0$	g	$\chi_2^{0*} \tilde{Y}^+ \tilde{\chi}^-$	$-g$
$\tilde{\chi}_2^0 \tilde{X} \chi_1^0$	g	$\chi_1^{0*} \tilde{X} \tilde{\chi}_2^0$	$-g$
$\tilde{\chi}_1^0 \tilde{X}^* \chi_2^0$	g	$\chi_2^{0*} \tilde{X}^* \tilde{\chi}_1^0$	$-g$
$\tilde{\rho}_1^+ \tilde{W}^- \rho^0$	g	$\rho^{0*} \tilde{W}^- \tilde{\rho}_1^+$	$-g$
$\tilde{\rho}_2^+ \tilde{Y}^- \rho^0$	g	$\rho^{0*} \tilde{Y}^- \tilde{\rho}_2^+$	$-g$
$\tilde{\chi}'^+ \tilde{W}^- \chi_1'^0$	$-g$	$\chi_1'^{0*} \tilde{W}^- \tilde{\chi}'^+$	g
$\tilde{\chi}'^+ \tilde{Y}^- \chi_2'^0$	$-g$	$\chi_2'^{0*} \tilde{Y}^- \tilde{\chi}'^+$	g
$\tilde{\chi}_2'^0 \tilde{X}^* \chi_1'^0$	$-g$	$\chi_1'^{0*} \tilde{X} \tilde{\chi}_2'^0$	g
$\tilde{\chi}_1'^0 \tilde{X} \chi_2'^0$	$-g$	$\chi_2'^{0*} \tilde{X} \tilde{\chi}_1'^0$	g
$\tilde{\rho}_1'^- \tilde{W}^+ \rho'^0$	$-g$	$\rho'^{0*} \tilde{W}^+ \tilde{\rho}_1'^-$	g
$\tilde{\rho}_2'^- \tilde{Y}^+ \rho'^0$	$-g$	$\rho'^{0*} \tilde{Y}^+ \tilde{\rho}_2'^-$	g

Vertex	factor	vertex	factor
$\mu_L \tilde{\mu}_L^c \tilde{\rho}^0$	$-iY_\mu$	$\tilde{\nu}_{\mu L} \tilde{\rho}_1^{\prime -} \mu_L^c$	$-iY_\mu$
$\tilde{\mu}_L \tilde{\rho}^0 \mu_L^c$	$-iY_\mu$	$\tilde{\nu}_{\mu L}^c \tilde{\rho}_2^{\prime -} \mu_L^c$	$-iY_\mu$
$\tau_L \tilde{\tau}_L^c \tilde{\rho}^0$	$-iY_\tau$	$\tilde{\nu}_{\tau L} \tilde{\rho}_1^{\prime -} \tau_L^c$	$-iY_\tau$
$\tilde{\tau}_L \tilde{\rho}^0 \tau_L^c$	$-iY_\tau$	$\tilde{\nu}_{\tau L}^c \tilde{\rho}_2^{\prime -} \tau_L^c$	$-iY_\tau$
$\mu_L \tilde{\rho}_2^+ \tilde{\nu}_{\tau L}$	$-2iY_{\nu_{\mu\tau}}$	$\mu_L \tilde{\rho}_1^+ \tilde{\nu}_\tau^c$	$2iY_{\nu_{\mu\tau}}$
$\tau_L \tilde{\rho}_2^+ \tilde{\nu}_{\mu L}$	$-2iY_{\nu_{\tau\mu}}$	$\tau_L \tilde{\rho}_1^+ \tilde{\nu}_{\mu L}^c$	$2iY_{\nu_{\tau\mu}}$

Table B.3

Higgsino-lepton-slepton interactions

$$-\frac{\lambda_{3ab}}{3} \left[l_{aL} \tilde{\rho}_2^+ \tilde{\nu}_{bL} - l_{aL} \tilde{\rho}_1^+ \tilde{\nu}_{bL}^c + \tilde{\nu}_{aL}^c \tilde{\rho}_1^+ l_{bL} - \tilde{\nu}_{aL} \tilde{\rho}_2^+ l_{bL} \right], \quad (\text{B.9})$$

From now we just note that because the conservation of lepton flavor in the lepton sector at tree level then $\lambda_{1ab} = 0$ with $a \neq b$ and $\lambda_{3cd} = 0$ with $c = d$. For simplicity, we use new notations: $Y_e \equiv \lambda_{111}/3$, $Y_\mu \equiv \lambda_{122}/3$, $Y_\tau \equiv \lambda_{133}/3$ and $Y_{\nu_{e\mu}} \equiv \lambda_{312}/3$, $Y_{\nu_{\mu\tau}} \equiv \lambda_{323}/3$, $Y_{\nu_{e\tau}} \equiv \lambda_{313}/3$. The Eq.(B.9) now can be written in the common form:

$$\begin{aligned} \mathcal{L}_{\tilde{u}\tilde{H}} = & -Y_\mu \left[\mu_L \tilde{\mu}_L^c \tilde{\rho}^0 + (\tilde{\nu}_{\mu L} \tilde{\rho}_1^{\prime -} + \tilde{\mu}_L \tilde{\rho}^0 + \tilde{\nu}_{\mu L}^c \tilde{\rho}_2^{\prime -}) \mu_L^c \right] \\ & -Y_\tau \left[\tau_L \tilde{\tau}_L^c \tilde{\rho}^0 + (\tilde{\nu}_{\tau L} \tilde{\rho}_1^{\prime -} + \tilde{\tau}_L \tilde{\rho}^0 + \tilde{\nu}_{\tau L}^c \tilde{\rho}_2^{\prime -}) \tau_L^c \right] \\ & -Y_{\nu_{ab}} [l_{aL} \tilde{\rho}_2^+ \tilde{\nu}_{bL} - l_{aL} \tilde{\rho}_1^+ \tilde{\nu}_{bL}^c + \tilde{\nu}_{aL}^c \tilde{\rho}_1^+ l_{bL} - \tilde{\nu}_{aL} \tilde{\rho}_2^+ l_{bL}] \end{aligned} \quad (\text{B.10})$$

Corresponding vertices are shown in Fig. B.3

(5) In the soft Langrangian, the mass term of sleptons is given by

$$\begin{aligned} \mathcal{L}_{\tilde{f}mass} = & -\tilde{m}_{Lab}^2 \tilde{L}_{aL}^\dagger \tilde{L}_{bL} - \tilde{m}_{Rab}^2 \tilde{l}_{aL}^{c*} \tilde{l}_{bL}^c - \left[h'_{ab} \tilde{L}_{aL}^T \rho' \tilde{l}_{bL}^c \right. \\ & + h_{ab} \varepsilon^{\alpha\beta\gamma} (\tilde{L}_{aL})_\alpha (\tilde{L}_{bL})_\beta (\rho)_\gamma + \frac{\lambda_{1ab}}{3} \mu_\rho \rho^* \tilde{L}_{aL} \tilde{l}_{bL}^c \\ & \left. + \frac{\lambda_{3ab}}{3} \mu_\rho \varepsilon^{\alpha\beta\gamma} (\rho'^*)_\alpha (\tilde{L}_{aL})_\beta (\tilde{L}_{bL})_\gamma + \text{H.c} \right], \end{aligned} \quad (\text{B.11})$$

here a, b are flavor indices $\{a, b = 1, 2, 3\}$ or $a, b = \{e, \mu, \tau\}$ and α, β, γ are component indices of $SU(3)_L$. The $\varepsilon^{\alpha\beta\gamma}$ is the antisymmetric tensor. In this paper we focus on the mixing of slepton $\tilde{\mu}$ and $\tilde{\tau}$. This mixing makes mass-eigenstate basis of slepton is different from [16]. For more detail, please see in the Appendix C. The Lagrangian relating with Higgs-lepton-slepton interactions has a form

$$\begin{aligned} \mathcal{L}_{\tilde{\mu}\tilde{\tau}H^0} = & - \left[(h'_{\mu\tau} \tilde{\mu}_L \rho^0 \tilde{\tau}_L^c + h'_{\tau\mu} \tilde{\tau}_L \rho^0 \tilde{\mu}_L^c + h'_\tau \tilde{\tau}_L^c \rho^0 \tilde{\tau}_L + h'_\mu \tilde{\mu}_L^c \rho^0 \tilde{\mu}_L) \right. \\ & \left. + \rho^0 (h_{\mu\tau} - h_{\tau\mu}) (\tilde{\nu}_{\mu L}^c \tilde{\nu}_{\tau L} - \tilde{\nu}_{\mu L} \tilde{\nu}_{\tau L}^c) + \frac{1}{2} Y_\tau \mu_\rho \rho^{0*} \tilde{\tau}_L \tilde{\tau}_L^c \right] \end{aligned}$$

vertex	factor	vertex	factor
$\tilde{\mu}_L^c \tilde{\mu}_L \rho'^0$	$-ih'_\mu$	$\tilde{\tau}_L^c \tilde{\tau}_L \rho'^0$	$-ih'_\tau$
$\tilde{\mu}_L \tilde{\tau}_L^c \rho'^0$	$-ih'_{\mu\tau}$	$\tilde{\tau}_L \tilde{\mu}_L^c \rho'^0$	$-ih'_{\tau\mu}$
$\rho^0 \tilde{\nu}_{\mu L}^c \tilde{\nu}_{\tau L}$	$-i(h_{\mu\tau} - h_{\tau\mu})$	$\rho^0 \tilde{\nu}_{\mu L} \tilde{\nu}_{\tau L}^c$	$i(h_{\mu\tau} - h_{\tau\mu})$
$\rho^0 \tilde{\tau}_L^* \tilde{\tau}_L^{c*}$	$-\frac{i}{2} Y_\tau \mu_\rho$	$\rho^0 \tilde{\mu}_L^* \tilde{\mu}_L^{c*}$	$-\frac{i}{2} Y_\mu \mu_\rho$
$\rho'^0 \tilde{\nu}_{\tau L}^* \tilde{\nu}_{\mu L}^{c*}$	$-i Y_{\nu_{\mu\tau}} \mu_\rho$	$\rho'^0 \tilde{\nu}_{\mu L}^* \tilde{\nu}_{\tau L}^{c*}$	$i Y_{\nu_{\mu\tau}} \mu_\rho$

Table B.4
slepton-slepton-Higgs vertices

$$+ \frac{1}{2} Y_\mu \mu_\rho \rho'^0 \tilde{\mu}_L \tilde{\mu}_L^c + Y_{\nu_{\mu\tau}} \mu_\rho \rho'^0 (\tilde{\nu}_{\tau L} \tilde{\nu}_{\mu L} - \tilde{\nu}_{\mu L}^c \tilde{\nu}_{\tau L}) + \text{H.c.}] \quad (\text{B.12})$$

Vertices of higgs- slepton-slepton interactions are listed in Fig. B.4

C Mass eigenstates of particles in the SUSYE331 model

C.1 Neutral Higgs

The physical states of Higgs (mass-eigenstates) have studied in [16]. For convenience we review the main results in this Appendix. First we expand the neutral Higgs components around the VEVs by

$$\begin{aligned} \chi^T &= \left(\frac{u+S_1+iA_1}{\sqrt{2}}, \chi^-, \frac{w+S_2+iA_2}{\sqrt{2}} \right); & \rho^T &= \left(\rho_1^+, \frac{v+S_5+iA_5}{\sqrt{2}}, \rho_2^+ \right) \\ \chi'^T &= \left(\frac{u'+S_3+iA_3}{\sqrt{2}}, \chi'^+, \frac{w'+S_4+iA_4}{\sqrt{2}} \right); & \rho'^T &= \left(\rho_1'^-, \frac{v'+S_6+iA_6}{\sqrt{2}}, \rho_2'^- \right) \end{aligned} \quad (\text{C.1})$$

where $\{u, w, u', w', v, v'\}$, $\{S_1, S_2, S_3, S_4, S_5, S_6\}$ and $\{A_1, A_2, A_3, A_4, A_5, A_6\}$ are VEV, scalar, and pseudo scalar parts of neutral higgs, respectively. The Higgs mass spectrum and the Higgs mass eigenstates given in [16] which showed that:

Scalar Higgs: Mass eigenstates of six original scalar higgs $\{S_1, S_2, S_3, S_4, S_5, S_6\}$ are defined as three massless eigenstates $\{S'_{1a}, S'_5, \varphi_{S_{24}}\}$ and three massive ones $\{\phi_{S_{24}}, \varphi_{S_{a36}}, \phi_{S_{a36}}\}$. The relations between the original and the mass-eigenstate base are ⁵:

⁵ There are some different definitions for γ in [15,16,17]. In this paper we use notations identifying with those of [15].

$$\begin{pmatrix} S_1 \\ S_2 \\ S_3 \\ S_4 \\ S_5 \\ S_6 \end{pmatrix} = \begin{pmatrix} c_\beta s_\theta & -s_\beta c_\theta & -c_\beta c_\theta & -s_\alpha s_\beta s_\theta & -c_\alpha s_\beta s_\theta & 0 \\ c_\beta c_\theta & s_\beta s_\theta & c_\beta s_\theta & -s_\alpha s_\beta c_\theta & -c_\alpha s_\beta c_\theta & 0 \\ s_\beta s_\theta & -c_\beta c_\theta & s_\beta c_\theta & s_\alpha c_\beta s_\theta & c_\alpha c_\beta s_\theta & 0 \\ s_\beta c_\theta & c_\beta s_\theta & -s_\beta s_\theta & s_\alpha c_\beta c_\theta & c_\alpha c_\beta c_\theta & 0 \\ 0 & 0 & 0 & -c_\alpha s_\gamma & s_\alpha s_\gamma & c_\gamma \\ 0 & 0 & 0 & c_\alpha c_\gamma & -s_\alpha c_\gamma & s_\gamma \end{pmatrix} \begin{pmatrix} S'_{1a} \\ \varphi_{S_{24}} \\ \phi_{S_{24}} \\ \varphi_{S_{a36}} \\ \phi_{S_{a36}} \\ S'_5 \end{pmatrix} \quad (C.2)$$

where some new notations are defined as the following:

$$t_\theta \equiv \tan \theta \equiv \frac{u}{w} = \frac{u'}{w'}, \quad c_\theta \equiv \cos \theta, \quad s_\theta \equiv \sin \theta,$$

$$t_\beta \equiv \tan \beta \equiv \frac{w}{w'}, \quad c_\beta \equiv \cos \beta, \quad s_\beta \equiv \sin \beta.$$

and

$$t_\gamma \equiv \tan \gamma \equiv \frac{v}{v'}, \quad s_\gamma \equiv \sin \gamma, \quad c_\gamma \equiv \cos \gamma.$$

and α is determined through relations:

$$\tan 2\alpha \equiv \frac{-2m_{36a}^2}{m_{66a}^2 - m_{33a}^2}, \quad c_\alpha \equiv \cos \alpha, \quad s_\alpha \equiv \sin \alpha$$

$$m_{33a}^2 = \frac{18g^2 + g'^2}{54c_\theta^2}(w^2 + w'^2) = \frac{(18g^2 + g'^2)w^2}{54c_\theta^2 s_\beta^2}$$

$$m_{66a}^2 = \frac{9g^2 + 2g'^2}{27}(v^2 + v'^2) = \frac{(9g^2 + 2g'^2)v^2}{27s_\gamma^2}$$

$$m_{36a}^2 = \frac{9g^2 + 2g'^2}{54} \sqrt{\frac{(v^2 + v'^2)(w^2 + w'^2)}{c_\theta^2}} = \frac{9g^2 + 2g'^2}{54} \frac{vw}{|c_\theta s_\gamma s_\beta|}$$

The mass eigenvalues of three physical Higgses $\phi_{S_{24}}$, $\varphi_{S_{a36}}$ and $\phi_{S_{a36}}$ are:

$$m_{\phi_{S_{24}}}^2 = \frac{g^2}{4}(1 + t_\theta^2)(w^2 + w'^2) = \frac{g^2 w^2}{c_\theta^2 s_\beta^2} \quad (C.3)$$

$$m_{\varphi_{S_{a36}}}^2 = \frac{1}{2} \left[m_{33a}^2 + m_{66a}^2 - \sqrt{(m_{33a}^2 - m_{66a}^2)^2 + 4m_{36a}^4} \right] \quad (C.4)$$

$$m_{\phi_{S_{a36}}}^2 = \frac{1}{2} \left[m_{33a}^2 + m_{66a}^2 + \sqrt{(m_{33a}^2 - m_{66a}^2)^2 + 4m_{36a}^4} \right] \quad (C.5)$$

Pseudo-scalar Higgs: There are five Goldstone bosons $\{A_5, A_6, A'_1, A'_2, \varphi_A\}$ and one massive physical Higgs φ_A . Because the φ_A does not receive any contributions from the A_5, A_6 and sleptons as well as their sneutrinos only couple to ρ, ρ' , hence there is no coupling of pseudo scalar φ_A to muon and tauon at the one loop approximation. This is the difference between MSMS and our model.

C.2 Mass eigenstates of sleptons

The masses of sleptons in SUSYE331 models were studied in details in [16]. In the work, they assumed that lepton numbers are conserved even in the slepton sector. This assumption led to the absence of mixing terms in slepton sector. Our work is interested in studying the source of LFV caused by the mixing between slepton $\tilde{\mu}$ and $\tilde{\tau}$ and ignore all other sources of FLV. So with two assumptions of R-parity conservation and the small left-right mixing in slepton sector, we can base on [16] to write the mass terms of charged sleptons in the form:

$$\begin{aligned}
-\mathcal{L}_{\tilde{l}^*} = & \sum_{\tilde{l}_{La}} \tilde{m}_{\tilde{l}_{La}}^2 \tilde{l}_{La}^* \tilde{l}_{La} + \left(\tilde{m}_{L_{\mu\tau}}^2 \tilde{\mu}_L^* \tilde{\tau}_L + \text{H.c.} \right) \\
& + \sum_{\tilde{l}_{Ra}} \tilde{m}_{\tilde{l}_{Ra}}^2 \tilde{l}_{Ra}^* \tilde{l}_{Ra} + \left(\tilde{m}_{R_{\mu\tau}}^2 \tilde{\mu}_R^* \tilde{\tau}_R + \text{H.c.} \right)
\end{aligned} \tag{C.6}$$

where $\tilde{l}_{La} = \{\tilde{e}_L, \tilde{\mu}_L, \tilde{\tau}_L\}$, $\tilde{l}_{Ra} = \{\tilde{e}_R, \tilde{\mu}_R, \tilde{\tau}_R\}$ and

$$\begin{aligned}
\tilde{m}_{\tilde{l}_{La}}^2 &\equiv B_{aa} = M_{aa}^2 + \frac{1}{4}\mu_{0a}^2 + \frac{v'^2}{18}\lambda_{1aa}^2 + \frac{1}{18}\lambda_{2a}^2(u^2 + w^2) \\
&\quad - \frac{g^2}{2} \left(H_3 - \frac{1}{\sqrt{3}}H_8 - \frac{2t^2}{3}H_1 \right), \\
\tilde{m}_{\tilde{l}_{Ra}}^2 &\equiv C_{aa} = m_{aa}^2 + \frac{v'^2}{18}\lambda_{1aa}^2 + g^2 t^2 H_1, \\
\tilde{m}_{L_{\mu\tau}}^2 &\equiv B_{23} = M_{23}^2 + \frac{1}{4}\mu_{02}\mu_{03} + \frac{1}{18}\lambda_{22}\lambda_{23}(u^2 + w^2), \\
\tilde{m}_{R_{\mu\tau}}^2 &\equiv C_{23} = m_{23}^2, \\
H_1 &\equiv \frac{1}{6} \left[(u^2 + w^2) \frac{\cos 2\beta}{s_\beta^2} - 2v^2 \frac{\cos 2\gamma}{s_\gamma^2} \right] \\
&= \frac{1}{6} \left[(u^2 + w^2) (\cot^2 \beta - 1) - 2v^2 (\cot^2 \gamma - 1) \right] \\
H_3 &\equiv -\frac{1}{4} \left[u^2 \frac{\cos 2\beta}{s_\beta^2} - 2v^2 \frac{\cos 2\gamma}{s_\gamma^2} \right] \\
&= -\frac{1}{4} \left[u^2 (\cot^2 \beta - 1) - 2v^2 (\cot^2 \gamma - 1) \right] \\
H_8 &\equiv -\frac{1}{4\sqrt{3}} \left[v^2 \frac{\cos 2\gamma}{s_\gamma^2} + (u^2 - 2w^2) \frac{\cos 2\beta}{s_\beta^2} \right], \\
&= \frac{1}{4\sqrt{3}} \left[v^2 (\cot^2 \gamma - 1) + (u^2 - 2w^2) (\cot^2 \beta - 1) \right],
\end{aligned}$$

$$t^2 \equiv \left(\frac{g'}{g} \right)^2 = \frac{6s_W^2}{3 - 4s_W^2} \quad (\text{C.7})$$

Note that here we use notations M_{aa}^2 and m_{aa}^2 in stead of m_{aL}^2 and m_{la}^2 in the soft breaking term of [15]. We assume that the mixing matrix of the $\tilde{\mu}_{L,R}$ and $\tilde{\tau}_{L,R}$ slepton masses is given by

$$- \mathcal{L}_{\tilde{\mu}\tilde{\tau}} = (\tilde{\mu}_L^*, \tilde{\tau}_L^*) \begin{pmatrix} \tilde{m}_{\mu L}^2 & \tilde{m}_{L\mu\tau}^2 \\ \tilde{m}_{L\mu\tau}^{*2} & \tilde{m}_{\tau L}^2 \end{pmatrix} \begin{pmatrix} \tilde{\mu}_L \\ \tilde{\tau}_L \end{pmatrix} + (\tilde{\mu}_L^{c*}, \tilde{\tau}_L^{c*}) \begin{pmatrix} \tilde{m}_{\mu R}^2 & \tilde{m}_{R\mu\tau}^2 \\ \tilde{m}_{R\mu\tau}^{*2} & \tilde{m}_{\tau R}^2 \end{pmatrix} \begin{pmatrix} \tilde{\mu}_L^c \\ \tilde{\tau}_L^c \end{pmatrix} \quad (\text{C.8})$$

This form is the same as that given in [4,5] (for detail, see [4], appendix A.1). Hence, the mass eigenstates and eigenvalues of sleptons in our model are similar to that in the MSSM [4,5]. In particular, the mass mixing matrix of the left handed and right handed of sleptons given in (C.8) produce the mass eigenstates such as $\{\tilde{l}_{L_2}, \tilde{l}_{L_3}\}$ and $\{\tilde{l}_{R_2}, \tilde{l}_{R_3}\}$. The corresponding mass eigenvalues are $\{\tilde{m}_{L_2}^2, \tilde{m}_{L_3}^2\}$ and $\{\tilde{m}_{R_2}^2, \tilde{m}_{R_3}^2\}$.

From now we adopt conventions the flavor states of sleptons are $\tilde{\mu}_L, \tilde{\tau}_L$ and $\tilde{\mu}_L^c, \tilde{\tau}_L^c$ while the mass eigenstates are $\tilde{l}_{L_2}, \tilde{l}_{L_3}$ and $\tilde{l}_{R_2}, \tilde{l}_{R_3}$, respectively. The relations between these two kinds of basics are: $\tilde{\mu}_L = c_L \tilde{l}_{L_2} - s_L \tilde{l}_{L_3}$, $\tilde{\tau}_L = s_L \tilde{l}_{L_2} + c_L \tilde{l}_{L_3}$, with $c_L = \cos \theta_L$, $s_L = \sin \theta_L$; $\tilde{\mu}_L^c = c_R \tilde{l}_{R_2} - s_R \tilde{l}_{R_3}$, $\tilde{\tau}_L^c = s_R \tilde{l}_{R_2} + c_R \tilde{l}_{R_3}$, with $c_R = \cos \theta_R$, $s_R = \sin \theta_R$. The mixing parameters satisfy the following relations:

$$s_L c_L = \frac{\tilde{m}_{L\mu\tau}^2}{\tilde{m}_{L_3}^2 - \tilde{m}_{L_2}^2}, \quad s_R c_R = \frac{\tilde{m}_{R\mu\tau}^2}{\tilde{m}_{R_3}^2 - \tilde{m}_{R_2}^2}. \quad (\text{C.9})$$

C.3 Sneutrinos

The general Lagrangian which gains masses for sneutrinos is given in [16] as the following

$$\mathcal{L}_{\tilde{\nu}} = \begin{pmatrix} \tilde{\nu}_{aL}^*, \tilde{\nu}_{aR}^* \end{pmatrix} \begin{pmatrix} A_{ab} & E_{ab} \\ E_{ab} & G_{ab} \end{pmatrix} \begin{pmatrix} \tilde{\nu}_{bL} \\ \tilde{\nu}_{bR} \end{pmatrix}, \quad (\text{C.10})$$

where

$$\nu_{aL} \equiv (\nu_{1L}, \nu_{2L}, \nu_{3L})^T, \quad \nu_{aR} \equiv \nu_{aL}^{c*} = (\nu_{1L}^{c*}, \nu_{2L}^{c*}, \nu_{3L}^{c*}), \quad (\text{C.11})$$

and

$$\begin{aligned}
A_{ab} &= \frac{g^2}{2} \delta_{ab} \left(H_3 + \frac{1}{\sqrt{3}} H_8 - \frac{2t^2}{3} H_1 \right) + M_{ab}^2 + \frac{1}{4} \mu_{0a} \mu_{0b}, \\
&\quad + \frac{1}{18} \lambda_{2a} \lambda_{2b} (v^2 + w^2) + \frac{2}{9} \lambda_{3ca} \lambda_{3cb} v^2, \\
G_{ab} &= -g^2 \delta_{ab} \left(\frac{1}{\sqrt{3}} H_8 + \frac{t^2}{3} H_1 \right) + M_{ab}^2 + \frac{1}{4} \mu_{0a} \mu_{0b}, \\
&\quad + \frac{1}{18} \lambda_{2a} \lambda_{2b} (v^2 + u^2) + \frac{2}{9} \lambda_{3ca} \lambda_{3cb} v^2, \\
E_{ab} &= -\frac{1}{\sqrt{2}} \left[(\varepsilon_{ab} - \varepsilon_{ba}) v + \frac{1}{6} \mu_\rho v' (\lambda_{3ab} - \lambda_{3ba}) \right]. \tag{C.12}
\end{aligned}$$

If the LFV happens only in the $\{\tilde{\nu}_\mu, \tilde{\nu}_\tau\}$ sector, we can rewrite the non-vanishing terms given in (C.12) in more explicit formulas:

$$\begin{aligned}
m_{\tilde{\nu}_{aL}}^2 &\equiv A_{aa} = \frac{g^2}{2} \left(H_3 + \frac{1}{\sqrt{3}} H_8 - \frac{2t^2}{3} H_1 \right) + M_{aa}^2 + \frac{1}{4} \mu_{0a}^2 \\
&\quad + \frac{1}{18} \lambda_{2a}^2 (v^2 + w^2) + \frac{2}{9} v^2 \sum_c \lambda_{3ca}^2, \\
m_{\tilde{\nu}_{aR}}^2 &\equiv G_{aa} = -g^2 \left(\frac{1}{\sqrt{3}} H_8 + \frac{t^2}{3} H_1 \right) + M_{aa}^2 + \frac{1}{4} \mu_{0a}^2 \\
&\quad + \frac{1}{18} \lambda_{2a}^2 (v^2 + u^2) + \frac{2}{9} v^2 \sum_c \lambda_{3ca}^2, \\
m_{\tilde{\nu}_{L\mu\tau}}^2 &\equiv A_{23} = M_{23}^2 + \frac{1}{4} \mu_{02} \mu_{03} + \frac{1}{18} \lambda_{22} \lambda_{23} (v^2 + w^2) + \frac{2}{9} v^2 \lambda_{3c2}^2 \lambda_{3c3}, \\
m_{\tilde{\nu}_{R\mu\tau}}^2 &\equiv A_{23} = M_{23}^2 + \frac{1}{4} \mu_{02} \mu_{03} + \frac{1}{18} \lambda_{22} \lambda_{23} (v^2 + u^2) + \frac{2}{9} v^2 \lambda_{3c2} \lambda_{3c3}. \tag{C.13}
\end{aligned}$$

Similar to the charged sleptons sector, we denote that $\{\tilde{\nu}_{\mu L}, \tilde{\nu}_{\tau L}, \tilde{\nu}_{\mu R}, \tilde{\nu}_{\tau R}\}$ as flavor eigenstates while $\{\tilde{\nu}_{L2}, \tilde{\nu}_{L3}, \tilde{\nu}_{R2}, \tilde{\nu}_{R3}\}$ as mass eigenstates. Also, notations $\{\tilde{m}_{\nu_{L2}}^2, \tilde{m}_{\nu_{L3}}^2, \tilde{m}_{\nu_{R2}}^2, \tilde{m}_{\nu_{R3}}^2\}$ are mass eigenstates of sneutrinos. Here the relations between two bases are:

$$\begin{aligned}
\tilde{\nu}_{\mu L} &= c_{\nu L} \tilde{\nu}_{L2} - s_{\nu L} \tilde{\nu}_{L3}, & \tilde{\nu}_{\tau L} &= s_{\nu L} \tilde{\nu}_{L2} + c_{\nu L} \tilde{\nu}_{L3}, \\
\tilde{\nu}_{\mu R} &= c_{\nu R} \tilde{\nu}_{R2} - s_{\nu R} \tilde{\nu}_{R3}, & \tilde{\nu}_{\tau R} &= s_{\nu R} \tilde{\nu}_{R2} + c_{\nu R} \tilde{\nu}_{R3}, \\
s_{\nu L} c_{\nu L} &= \frac{\tilde{m}_{\nu_{L\mu\tau}}^2}{\tilde{m}_{\nu_{L3}}^2 - \tilde{m}_{\nu_{L2}}^2}, & s_{\nu R} c_{\nu R} &= \frac{\tilde{m}_{\nu_{R\mu\tau}}^2}{\tilde{m}_{\nu_{R3}}^2 - \tilde{m}_{\nu_{R2}}^2}, \tag{C.14}
\end{aligned}$$

References

- [1] The ATLAS Collaboration (G. Aad et al.). Jan 2009. 1852 pp, arXiv:0901.0512.
- [2] ILC Collaboration (Gerald Aarons (SLAC) et al.). Sep 2007, arXiv:0709.1893.
- [3] E. Arganda, A. M. Curiel, M. J. Herrero, D. Temes, Phys. Rev. D **71** (2005) 035011, arxiv: 0407302.
- [4] A. Brignoble, A. Rossi, Phys. Lett. **B 66** (2003) 217, arXiv:0304081.
- [5] A. Brignole, A. Rossi, Nucl. Phys. **B 701** (2004),3-53, arXiv: 0404211.
- [6] J. L. Diaz-Cruz, D. K. Gosh and S. Morreti, Phys. Lett. **B 679** (2009) 376, arXiv:0809.5158.
- [7] K. S. Babu and C. Kolda, Phys. Lett **B 451** (1999) 77, arxiv: 9811308.
- [8] K. S. Babu and C. Kolda, Phys. Rev. Lett. **89** (2002) 241802, arXiv: 0206310; K. S. Babu and C. F. Kolda, Phys. Rev. Lett. **84** (2000) 228, e-Print: hep-ph/9909476.
- [9] J. Guasch, W. Hollik and S. Penaranda, Phys. Lett. **B 515** (2001) 367, arxiv: 0106027.
- [10] M. Cannoni and O. Panella, Phys. Rev. D **79** (2009) 056001, Arxiv: 0812.2875; Phys. Rev. D **81** (2010) 036009, arXiv:0910.3316; Nuovo Cim. **C 33** (2010) 183, arXiv:1002.3697.
- [11] M. S. Carena, D. Garcia, U. Nierste and C. E. M. Wagner, Nucl. Phys. **B 577** (2000) 88, arXiv: 9912516.
- [12] T. Goto, Y. Okada and Y. Yamamota, Phys. Rev. D **83** (2011) 053011, arXiv:1012.4385.
- [13] T. Blazek and S. Raby, Phys. Rev. D **59** (1999) 095002, Arxiv: 9712257.
- [14] G. Isidori and A. Retico, JHEP **0111** (2001) 001, Arxiv: 0110121.
- [15] P. V. Dong, D. T. Huong, M. C. Rodriguez, H. N. Long, Nucl. Phys. **B 772** (2007) 150; e-Print: hep-ph/0701137.
- [16] P. V. Dong, Tr. T. Huong, N. T. Thuy and H. N. Long, JHEP **0711** (2007)073, arXiv:0708.3155 [hep-ph].
- [17] P. V. Dong, D. T. Huong, N. T. Thuy and H. N. Long, Nucl. Phys. **B 795** (2008) 361; arXiv:0707.3712
- [18] D. T. Huong and H. N. Long, JHEP **0807** (2008) 049, arXiv:0804.3875.
- [19] P. V. Dong, H. N. Long, D. T. Nhung, D. V. Soa, Phys. Rev. D **73**, 035004 (2006), P. V. Dong, H. N. Long, Adv. High Energy Phys., **2008**, 739492 (2008); arXiv: 0804.3239; W. Ponce, Y. Giraldo, L. A. Sanchez, Phys. Rev. D **67**, 075001 (2003).

- [20] D. Atwood, L. Reina and A. Soni, Phys. Rev D **55**, 3156 (1997)
- [21] P. Paradisi, JHEP **0608** (2006) 047, e-Print: hep-ph/0601100.
- [22] J. L. Diaz-Cruz, JHEP **0305** (2003) 036, e-Print: hep-ph/0207030.
- [23] Y. Okada, K. Okumura, Y. Shimizu, Phys.Rev. D **61** (2000) 094001, e-Print: hep-ph/9906446.
- [24] Y. Miyazaki *et al.* [Belle Collaboration], Phys. Lett. **B 660** (2008) 154, arXiv:0711.2189.
- [25] J. Hisano and D. Nomura, Phys. Rev. D **59**, 116005 (1999), International Workshop on Nuclear and Particle Physics at J-PARC (NP08), Mito, Ibaraki, Japan, March, 2008 (<http://j-parc.jp/NP08/>).
- [26] J. C. Montero, V. Pleitez, M. C. Rodriguez, Phys. Rev. D **70** (2004) 075004.